A STUDY OF THE INTRODUCTION OF IONS INTO THE REGION OF STRONG FIELDS WITHIN A QUADRUPOLE MASS SPECTROMETER

By

WILSON M. BRUBAKER

BELL & HOWELL RESEARCH CENTER
360 SIERRA MADRE VILLA
PASADENA, CALIFORNIA

CONTRACT NASW-1298

FIFTH
QUARTERLY PROGRESS REPORT
for the period
17 AUGUST 1966 THROUGH 17 NOVEMBER 1966

NATIONAL AERONAUTICS AND SPACE ADMINISTRATION
WASHINGTON, D.C.

A STUDY OF THE INTRODUCTION OF IONS INTO THE REGION OF STRONG FIELDS WITHIN A QUADRUPOLE MASS SPECTROMETER

by

Wilson M. Brubaker

ABSTRACT

This project is a theoretical and experimental study of the introduction of ions into the strong fields of a quadrupole mass filter. The performance of a conventional quadrupole has been compared to that of one with a lower ratio of dc to ac fields in the entrance region for a wider range of ion injection energies. The superior performance of the delayed dc mode of operation is well documented. Computations have been made of the trajectories as the ions leave the quadrupole field. These show that the termination of the field should be as abrupt as possible, or a delayed ac ramp used to prevent large radial accelerations of the ions. A system for making careful comparisons of the performance of quadrupoles with round and hyperbolic rod structures has been assembled and put into operation.

TABLE OF CONTENTS

LIST OF TABLE AND FIGURES

Table

Figures

Figures

INTRODUCTION

This report covers the work done by the Bell & Howell Research Center on NASA Contract NASW-1298 from 17 August through 17 November 1966. This is the fifth quarter of the Contract.

This project is concerned with the introduction of ions into the region of strong fields in the quadrupole mass filter, and with the comparison of the performances of quadrupole structures with round and with hyperbolic field-forming surfaces.

The investigation of the influence of delayed dc ramp mode of operation has been extended to include widely varying ion injection energies, and is essentially concluded with this report. A preliminary report of these studies was made at the October meeting of the American Vacuum Society in San Francisco.

A system for testing the operation of quadrupoles with round and hyperbolic rod shapes has been very carefully designed, fabricated and assembled. Careful attention has been given to keeping the aberrations in the contours of the field-forming surfaces quite low. Extensive refinements have been made in the electronic circuitry used to energize the apparatus.

THEORETICAL

Computer Studies

Because of the large radial components of velocity which the ions acquire as they respond to the strong electric fields within the quadrupole, it is anticipated that they leave the end of the quadrupole with high velocities, randomly directed. This condition makes it virtually impossible to focus the emerging beam with electrostatic lenses, using convenient potentials.

It is important to learn what, if any, reduction can be made in the magnitude of the random velocities of the emerging ions by appropriately terminating the fields at the exit of the quadrupole. To this end, trajectories have been computed for a variety of field terminations. Previous computations have shown that, for a set of a-q values which correspond to a resolving power of about 400, the envelopes to the x- and y-trajectories reach maximum amplitudes when $\omega t = 140$.

In the studies of field terminations the fields are assumed to be of full value for $0 \leq \omega t \leq 140$ radians. The terminations begin when $\omega t = 140$, $140 + \pi/2$, and $140 + \pi$. The various phase angles at which the terminations begin were chosen because it was suspected that the phase of the ac potential has a considerable influence on the trajectories.

The first series of computations assume a conventional quadrupole termination, in which the ratio of the dc to the ac potentials is everywhere the same. Three lengths of field ramp terminations are assumed: two, six, and ten cycles long. In the second series the dc field is assumed to decrease to zero before the ac. This is done in two different manners, but in each case all fields go to zero in an interval of ten cycles. In the first manner the dc field decays during five cycles, and then the ac decays during the following five cycles. In the second manner the dc is assumed to decay during two cycles, and the ac field, during the following eight cycles.

Figures 1 to 10 show the detailed trajectories, with the nearly sinusoidal response indicated by straight lines drawn between points of reversal. The influence of the phase of the ac potentials at the time the field termination begins is apparent, but is not as dominant as anticipated. It is interesting to note that the conditions at the exit end of the quadrupole are similar to those at the entrance. That is, for the coincident ramp of the conventional quadrupole, an appreciable weakening of the fields makes the trajectory unstable in the y-direction. In the x-direction the stability is increased and the amplitudes of the trajectories, in general, become less.

Figures 11 to 15 are on a quite different scale, to show the relative magnitudes of the exit velocities of the ions under the different field terminations. In these figures the trajectories of the ions after they leave the fringe fields are shown. In each case the axial velocity of the ions is assumed to be constant, so that the z-distance increases linearly with time. Thus the ωt axis is completely analogous to the z axis of the instrument.

The normalized, dimensionless components of radial velocity are tabulated in Table I. The velocity is in terms of $(r/r_0)/(\omega t)$. These data, and the corresponding graphic display of the trajectories, indicate quite clearly the important conclusions which can be drawn from this investigation. They are:

1. When the field termination is abrupt the ions leave the quadrupole with radial velocities which are 30% to 40% as large as those with which they respond to the fields within the quadrupole.

2. If the termination is gradual, very large components of velocity are added to the y-component of motion.

3. The x-component of velocity is usually less than a third of the normal radial velocity within the quadrupole under almost all conditions of field terminations.

4. When the dc fields are attenuated ahead of the ac fields, the x- and the y-components of velocity become quite small, much less than their normal velocities within the quadrupole.

For circumstances in which it is desired to apply any kind of ion optics to direct the ions from the quadrupole to a remote detector, the use of the delayed ac ramp becomes of prime importance.

EXPERIMENTAL

General Discussion

During the previous quarters, data have been obtained which relate the sensitivity of the system to the resolving power for the two modes of operation, conventional and delayed dc ramp. It was discovered that the energy of the incident ions is an important parameter in this investigation. During the present quarter this investigation has been continued, using ion energy as one of the variables. Data are now available for ion energies from 4 to 15 volts, inclusive.

The relationship between the number of cycles which occur during the passage of ions through the fringing field and the maximum amplitude of the resulting trajectory was computed during the last quarter. It was found that the amplitude increases exponentially with the number of cycles. The importance of minimizing the number of cycles spent in the fringe field of the conventional quadrupole was not fully appreciated before these computations were made.

The intial experimental data relating sensitivity to resolving power for the two modes of operation were obtained under conditions which were less than ideal for properly evaluating the importance of using the delayed mode. First, the source was mounted an inch away from the quadrupole and the entrance aperture was large, half the rod diameter. This geometry provided a large leakage field and increased the number of cycles required for an ion to traverse it. This circumstance favors the delayed ramp mode of operation. On the other hand, a rather high, 15 volt, ion injection energy was used. This reduces the number of cycles and favors the conventional mode, as far as the entrance conditions are concerned. For the experiments of last quarter and this quarter, the ion source has been placed adjacent to the quadrupole. Under these conditions, the advantages of the delayed dc ramp mode are more apparent at the lower ion injection energies.

The fields in the quadrupole are entirely radial. Thus the length of the quadrupole serves only to permit the ions to remain in the radial fields for the length of time required to achieve the desired mass resolution. The slower the ions move during their transit, the greater the number of cycles which occur during their passage. However, the results of this study, both theoretical and experimental, show that the transmission efficiency for the ions suffers tremendously if low velocity ions are introduced into the conventional quadrupole. This severe limitation is nonexistent for the delayed mode of operation.

The number of cycles an ion needs to spend in the radial fields for a given resolving power was found by Paul to be

$$n \geq 5\ (m/dm) \tag{1}$$

for resolving power calculated near the base of the peak. Obviously, n is also equal to the excitation frequency times the transit time, or

$$n = f(L/v) \tag{2}$$

where L is the quadrupole length, centimeters, f the excitation frequency, megahertz, and v the axial velocity, centimeters per microsecond. A combination of equations (1) and (2) yields the following expression for the limiting resolving power:

$$m/dm = L^2 f^2 m/50\ V_i \tag{3}$$

where V_i is the potential through which the ions are accelerated before they enter the quadrupole, and m is the mass of the ion, in atomic mass units.

Experimental Data

The above considerations reveal the necessity of making sensitivity-vs-resolving power measurements at various ion injection energies. This has been done. The data of the fourth quarter have been extended to include ion energies of 8 and 11 volts. Data are now available for ion injection energies of 4, 6, 8, 11, and 15 volts. These data are presented in Figures 16 and 17.

The data which have been assembled relating the instrument sensitivity to resolving power for the conventional and the delayed dc ramp mode of operation dramatically reveal the importance of incident ion energy. Before discussing in detail the differences between the plots of Figures 16 and 17, it should be noticed that the efficiency of the ion source is voltage dependent. This is most readily recognized in the data of Figure 17 for the delayed dc ramp mode of operation. At low resolving power the sensitivity has only a weak dependence on the resolving power. If it is assumed that ions traverse the fringe fields without appreciable loss in this case, then the differences in sensitivity at different ion injection energies is attributable to varying source efficiencies. Over the range of ion injection energies used in these experiments, this source efficiency variation may be as large as a factor of ten, as suggested by the data of Figure 17. Similar data from Figure 16 for the conventional quadrupole show a 200-fold attenuation of the sensitivity as the ion injection energy is lowered from 15 to 4 volts. Thus the attenuation is at least 20 times as much for the conventional mode. This again is indicative of the severity of the loss of ions owing to their passage through the fringe fields of the conventional quadrupole.

The data of Figure 16 for the conventional quadrupole indicate the great loss of sensitivity as the energy of the incident ions is reduced. As mentioned before, this is due in part to a lowered source efficiency. The greater portion of the loss is due to the ions' traversal of the fringe fields. Note also the approach to limiting resolving power at the higher ion energies. This occurs because the ions spend insufficient time in the quadrupole. These data show rather dramatically how the combination of high sensitivity and high resolving power is impossible to obtain with the conventional quadrupole. At low ion injection energy the loss is due to fringe field effects, and at high injection energy it is due to too few cycles being spent during the transit of the ion through the quadrupole.

The data of Figure 17 for the delayed dc ramp mode of operation show a quite different dependence of sensitivity on ion injection energy. Comparing first the limiting resolving power at 15 volt injection energy, it is noted that the resolving power of the conventional quadrupole exceeds slightly that of the delayed dc ramp quadrupole. Here is an example of the operating conditions in which equation (3) applies.

$$m/dm = L^2 f^2 m/50\ V_i \qquad (3)$$

The resolving power at the constant sensitivity is limited by the number of cycles the ions spend in the mass resolving portion of the quadrupole. The effective mass resolving length of the quadrupole is shorter for the delayed dc ramp mode because the rod segment is not at full dc potential. The segment length, 0.6 inches, is 6% of the rod length. Thus the conventional quadrupole would be expected to have a 12% higher limit to its resolving power, as indicated by equation (3). Experimentally, the advantage is less than 12%.

The sensitivity at resolving powers below 300 for the delayed dc ramp quadrupole has only a modest dependence on the ion injection energy, as shown in Figure 17. As mentioned earlier, this variation is attributed largely to ion source phenomena. At resolving powers above 300 the influence of ion injection energy is of major importance. In particular, the limiting resolving power at reduced sensitivity is very much a function of the injection energy. The resolving power appears to be limited by the time spent by the ions in the analyzer.

In the quadrupole mass spectrometer, as in all other mass analyzers, higher resolving power is obtained at the expense of sensitivity. It is interesting to compare the operation of the quadrupole in the two modes when the resolving power has been pushed near its ultimate, and the sensitivity has suffered severely. In Figure 18 the resolving power for operation in the two modes is presented as functions of the ion injection energy, at a constant sensitivity of 10^{-7} amps/torr. Data for the delayed mode are most readily interpreted. Equation (3) shows that the resolving power capability of the instrument varies inversely with the ion injection energy. Figure 18 shows the resolving power to fall continuously with an increase in ion injection energy, but less fast than the inverse power suggested by equation (3). This lack of agreement is due to the fact that other operating parameters are functions of the injection energy, too. Earlier, the source efficiency was mentioned as one of these parameters. The relation between resolving power and ion energy for the delayed mode as seen in Figure 18 agrees qualitatively with the prediction of theory.

Ion Source Studies

Quadrupole mass filters differ drastically from magnetic types in their source requirements. Magnetic mass separators need line sources of high intensity. Quadrupole mass separators have circular entrance apertures and for optimum operating conditions accept ions from the entire aperture. Previous experience and the computer data of this study show that, for the conventional quadrupole, the ions should be introduced near the axis. Guided by experience, we had previously designed an ion source of nearly circular symmetry. This is a very good source, and when used on a ten-inch quadrupole with a secondary emission multiplier permits the display of peaks at a partial pressure of 2 x 10^{-14} amperes. However, the data of the present experiment indicate that the sensitivity of the source, amperes per torr, is considerably lower than that claimed for sources of other designs. However, it should be kept in mind that the more significant figure-of-merit is the signal-to-noise ratio, not amperes per torr. The former figure alone determines the lowest molecular density to which the system is responsive.

The geometry of the source is shown in Figure 19. The filament nearly surrounds the ionizing region. The radial flow of electrons results in a maximum density of the electrons near the axis of the source, causing the ion production rate also to be maximized near the axis. "Noise" signal in a system with a secondary emission multiplier can be the result of photons striking the elements of the multiplier. Photons in an ion source originate at the electrodes struck by the electrons at the end of their path. This source has been designed so that there is no line-of-sight path between the multiplier and any surface that can be struck by an electron. This consideration has been found to be of extreme importance in keeping the signal-to-noise ratio at a minimum value.

The first investigation directed toward the improvement of this source concerned the distribution of electron current among the electrodes. The ion current output of the source was also obtained as a function of the potential of the various electrodes. The data obtained during the variation of the potential of electrode seven is of particular interest. The distribution of the electron current is shown in Figure 20, and the corresponding ion current in Figure 21. The electron current distribution is interesting, and rather normal. However, the sharp dependence of the ion current on the potential of electrode seven was not anticipated. In particular, the increase in output at positive potentials is anomalous. It was deduced that this increased ion current results from the production of ions in the portions of the source remote from the quadrupole. To prove this conclusion, the geometry of the source was altered as shown in Figure 22. A cylindrical tube has been added to electrode six which effectively shields the ionizing region from the potential of the adjacent portions of electrode seven. This change made little difference in the distribution of the electron currents, but it made a big difference in the ion current output, as seen in Figure 23. This refinement increased the sensitivity of the source by a factor of two.

Through the addition of an independent variation of the potential of electrode six (it had been connected to electrode five) the sensitivity of the source is increased by an additional factor of two. These two refinements increased the sensitivity by a factor of four. There should be no concurrent increase in the noise signal at the output of the multiplier by these changes, but it has not been measured.

This increase in the sensitivity of the ion source means that the previous data of amperes per torr can all be increased by a factor of four.

New Apparatus

The system for comparing the performance of round and hyperbolic field-forming surfaces has been assembled. The design goals for the controls and the manner in which the quadrupoles were fabricated were described in last quarter's report. Further descriptions of the electronic portion will be given next quarter, after the apparatus has been used.

A few photographs of the quadrupole assemblies are included in this report. Figure 24 shows the partially disassembled apparatus. The circular ion sources are seen with their electrical leads. These leads attach to pins which protrude from the support structure, and which are visible at about the seven-o'clock position. The inner ends of these pins are connected to the pins of the bakeable feed-through plugs. The ends of the field-forming electrodes (rods) are visible. They appear as 110° arcs, and are brought to the front of the support structure. This extension of the rods results in short field-ramps for the entrance region. Portions of the Venetian blind secondary emission multipliers are visible. The potential dividers are contained within the vacuum wall, thus reducing the number of feed-through connections required. Suitably made external connections permit the use of the entire multiplier assembly as a Faraday Cage collector. A high impedance feed-through at the rear of the vacuum wall conducts the ion current signal directly to electrometer assembly which attaches directly to the quadrupole.

Figure 25 is a photograph of the two sets of rods. Note that 110° extensions are to be found at each end of each rod. The extension at the ion exit end permits close proximity of the multiplier to the quadrupole, and gives high ion collection efficiency when the multiplier assembly is used as a Faraday Cage. Figure 26 is a close-up of the front ends of rods of the two types. The departure of the hyperbolic surface from a circle is most evident in the thickness of the rod extension. On the round rod, the thickness of the extension is uniform. The ceramic spacer which serves both as a support member and as an electrical insulator is clearly seen in each rod.

CONCLUSIONS

A theoretical study of the ion trajectories at the exit end of the quadrupole reveals the desirability of making the distance from the end of the quadrupole to the Faraday Cage as short as is convenient. As anticipated, the velocity vectors of emerging ions are quite randomly distributed both in direction and in magnitude. Since this represents such a "hot" source of ions, it is most difficult to concentrate them through the use of ion optics. Uncomfortably high potentials would be required to overcome this handicap.

The experimental investigation of the sensitivity vs. resolving power data have been extended to include wide variations in the energy of the injected ions. The factors which have dominant influence on the performance of the conventional quadrupole are much better understood as a result of these studies.

Preliminary ion source studies have improved the sensitivity by a factor of four without an apparent increase in the noise at the collector.

The system for evaluating the performance of a quadrupole with the usual round rods with that of a quadrupole with hyperbolic field-forming surfaces has been completely assembled, and is ready for operation.

NEXT QUARTER'S ACTIVITIES

During the next quarter data will be obtained comparing the round and the hyperbolic quadrupoles. The apparatus for this experiment is entirely assembled, and is ready for operation.

Source investigations will be continued, using different geometries.

TABLE I.

RADIAL COMPONENT OF VELOCITIES OF IONS AS THEY LEAVE THE QUADRUPOLE

TERMINATION RAMP CONFIGURATIONS				ESCAPE VELOCITY	
Phase	Fields, % DC	Fields, % AC	Figures Legend	$100(x/r_o)/\omega t$	$100(y/r_o)/\omega t$
0 to 140	100	100	1, 2, 11	- 5.3	+ 5.1
140 + 4π	0	0	——— X1, Y1		
0 to 140 + π/2	100	100	1, 2, 11	- 7.8	+ 3.3
140 + 4.5π	0	0	— — X2, Y2		
0 to 140 + π	100	100	1, 2, 11	- 7.6	+ 3.9
140 + 5π	0	0	- - - X3, Y3		
0 to 140	100	100	3, 4, 12	- 0.17	+ 54
140 + 12π	0	0	——— X4, Y4		
0 to 140 + π/2	100	100	3, 4, 12	- 4.2	+ 49
140 + 12.5π	0	0	— — X5, Y5		
0 to 140 + π	100	100	3, 4, 12	- 5.5	+ 50
140 + 13π	0	0	- - - X6, Y6		
0 to 140	100	100	5, 6, 13	+ 2.7	+540
140 + 20π	0	0	——— X7, Y7		
0 to 140 + π/2	100	100	5, 6, 13	- 1.1	+510
140 + 20.5π	0	0	— — X8, Y8		
0 to 140 + π	100	100	5, 6, 13	- 4.2	+513
140 + 21π	0	0	- - - X9, Y9		
0 to 140	100	100	7, 8, 14	- 2.9	+ 0.22
140 + 10π	0	100	——— X10, Y10		
140 + 20π	0	0			
0 to 140 + π/2	100	100	7, 8, 14	- 3.5	- 0.18
140 + 10.5π	0	100	— — X11, Y11		
140 + 20.5π	0	0			
0 to 140 + π	100	100	7, 8, 14	- 2.9	- 0.17
140 + 11π	0	100	- - - X12, Y12		
140 + 21π	0	0			

TERMINATION RAMP CONFIGURATIONS				ESCAPE VELOCITY	
Phase	Fields, % DC	Fields, % AC	Figures Legend	$100(x/r_o)/\omega t$	$100(y/r_o)/\omega t$
0 to 140	100	100	9, 10, 15	- 2.2	- 2.64
$140 + 4\pi$	0	100	______ X13, Y13		
$140 + 20\pi$	0	0			
0 to $140 + \pi/2$	100	100	9, 10, 15	+ 0.66	- 3.14
$140 + 4.5\pi$	0	100	— — X14, Y14		
$140 + 20.5\pi$	0	0			
0 to $140 + \pi$	100	100	9, 10, 15	+ 3.8	- 2.9
$140 + 5\pi$	0	100	- - - X15, Y15		
$140 + 21\pi$	0	0			

Approximate maximum velocity of ions in quadrupole 24 12

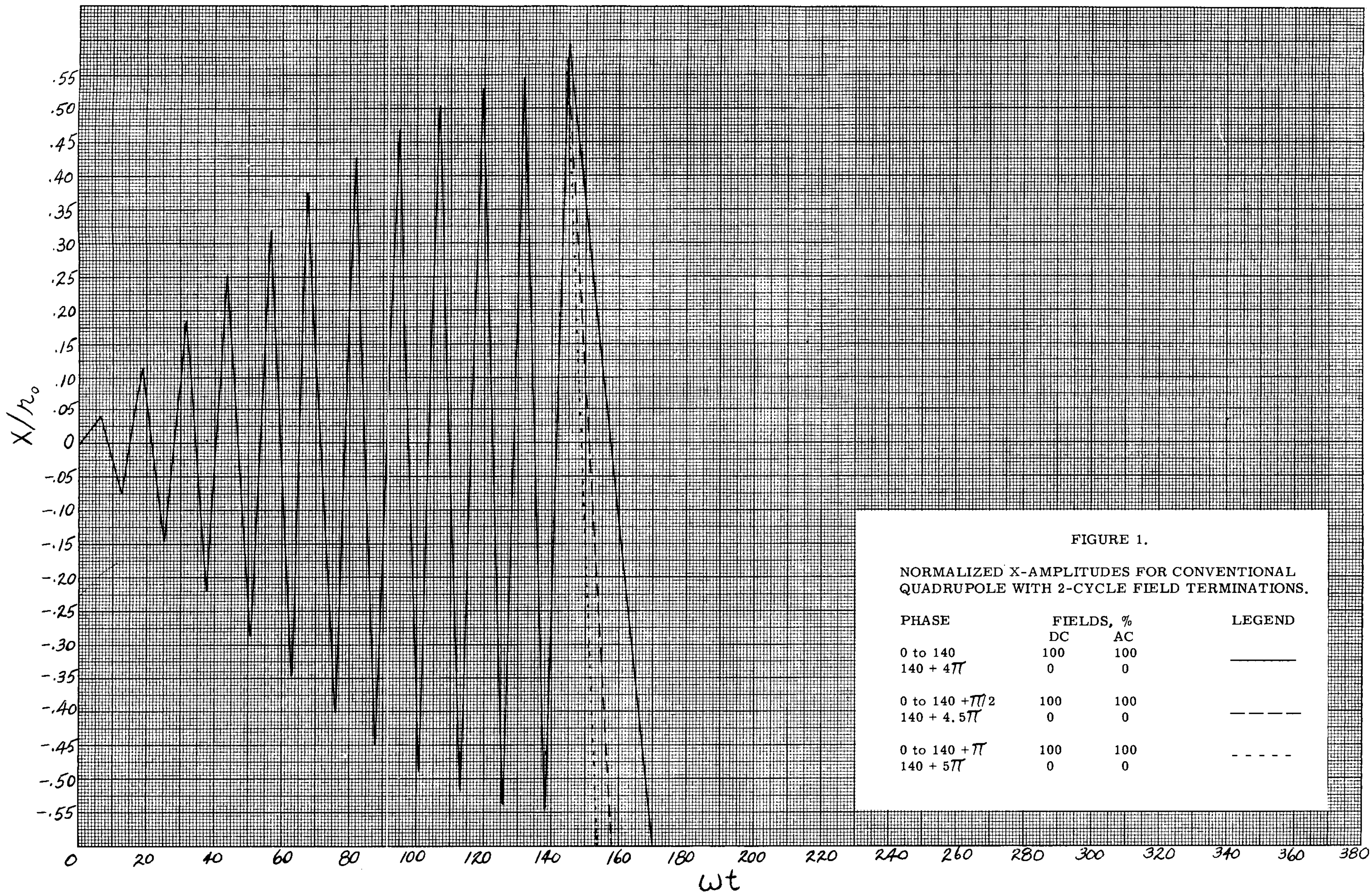

FIGURE 1.

NORMALIZED X-AMPLITUDES FOR CONVENTIONAL QUADRUPOLE WITH 2-CYCLE FIELD TERMINATIONS.

PHASE	FIELDS, % DC	FIELDS, % AC	LEGEND
0 to 140	100	100	————
140 + 4π	0	0	
0 to 140 + π/2	100	100	— — — —
140 + 4.5π	0	0	
0 to 140 + π	100	100	- - - - -
140 + 5π	0	0	

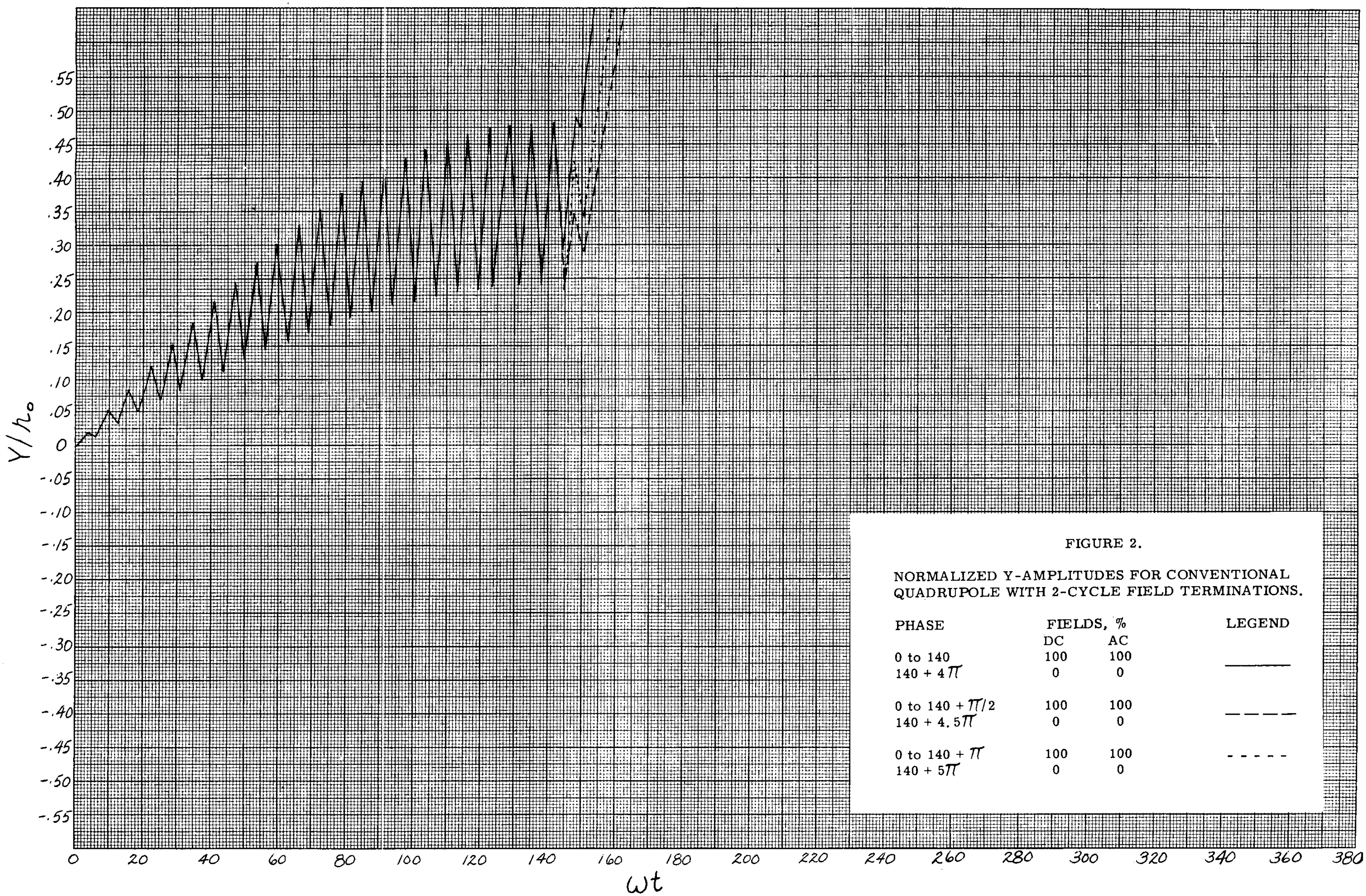

FIGURE 2.

NORMALIZED Y-AMPLITUDES FOR CONVENTIONAL QUADRUPOLE WITH 2-CYCLE FIELD TERMINATIONS.

PHASE	FIELDS, % DC	AC	LEGEND
0 to 140	100	100	————
140 + 4π	0	0	
0 to 140 + π/2	100	100	— — — —
140 + 4.5π	0	0	
0 to 140 + π	100	100	- - - - -
140 + 5π	0	0	

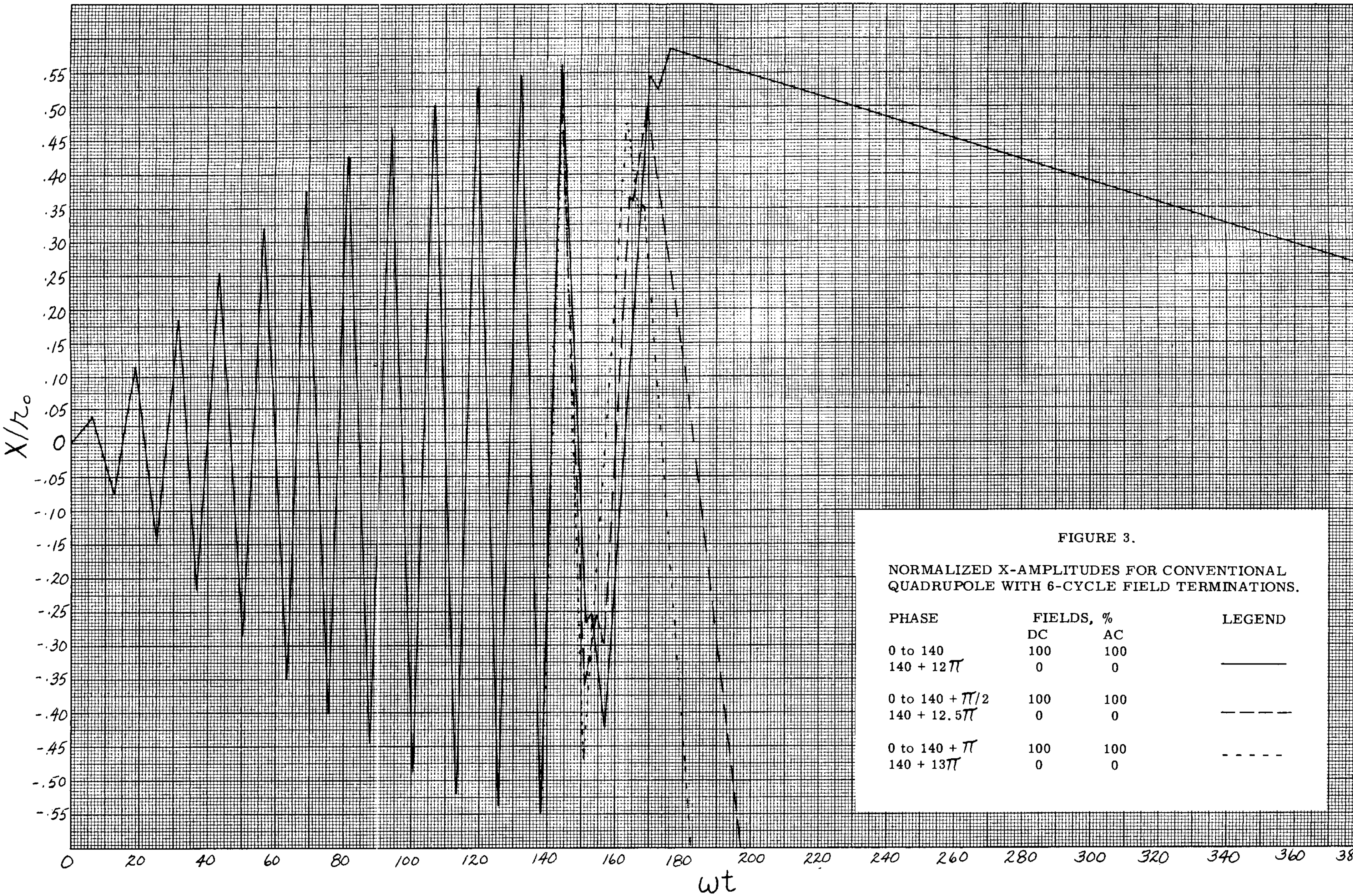

FIGURE 3.

NORMALIZED X-AMPLITUDES FOR CONVENTIONAL QUADRUPOLE WITH 6-CYCLE FIELD TERMINATIONS.

PHASE	FIELDS, % DC	AC	LEGEND
0 to 140	100	100	————
140 + 12π	0	0	
0 to 140 + π/2	100	100	— — — —
140 + 12.5π	0	0	
0 to 140 + π	100	100	- - - - -
140 + 13π	0	0	

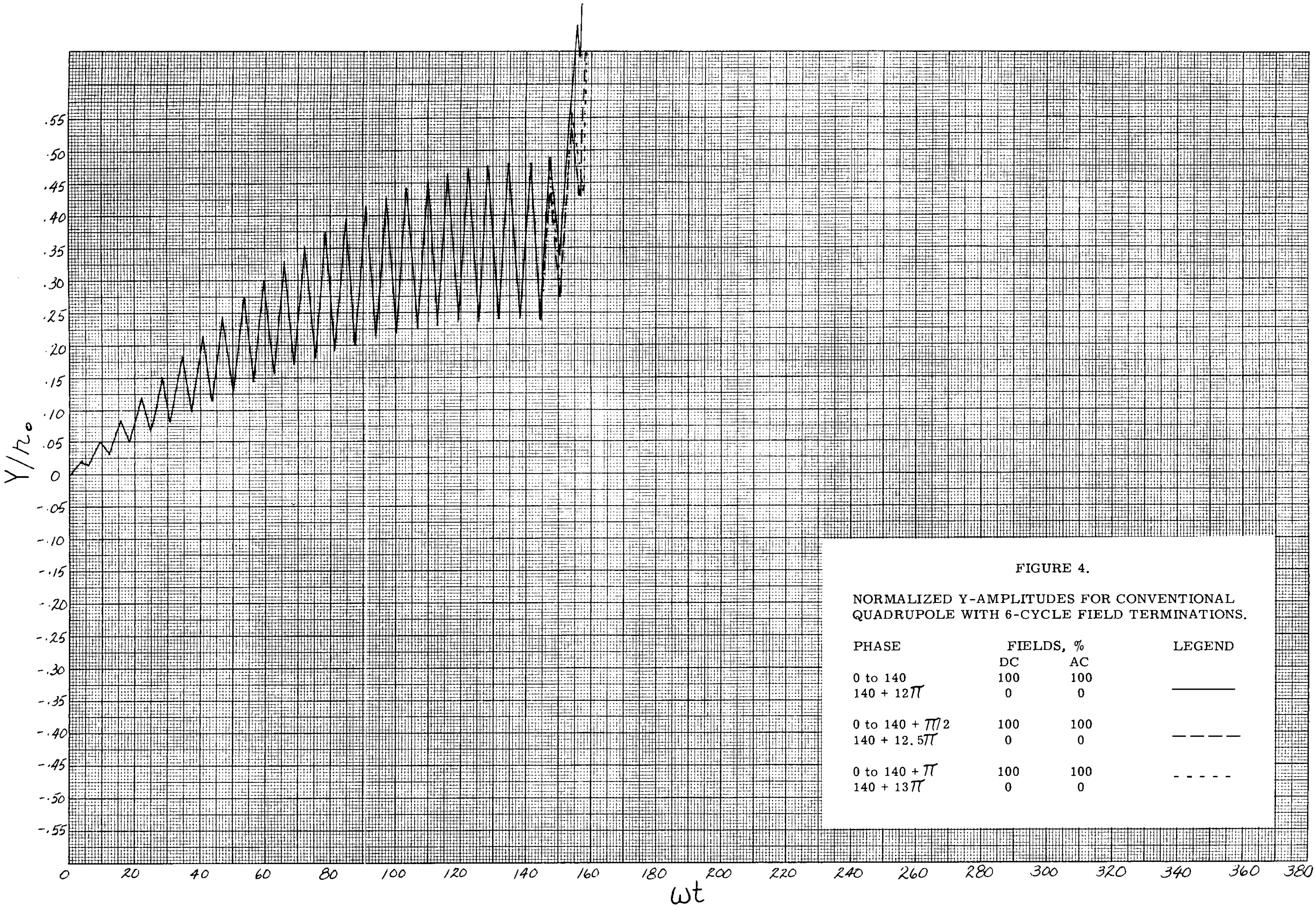

FIGURE 4.

NORMALIZED Y-AMPLITUDES FOR CONVENTIONAL QUADRUPOLE WITH 6-CYCLE FIELD TERMINATIONS.

PHASE	FIELDS, % DC	AC	LEGEND
0 to 140	100	100	———
140 + 12π	0	0	
0 to 140 + $\pi/2$	100	100	— — — —
140 + 12.5π	0	0	
0 to 140 + π	100	100	- - - - -
140 + 13π	0	0	

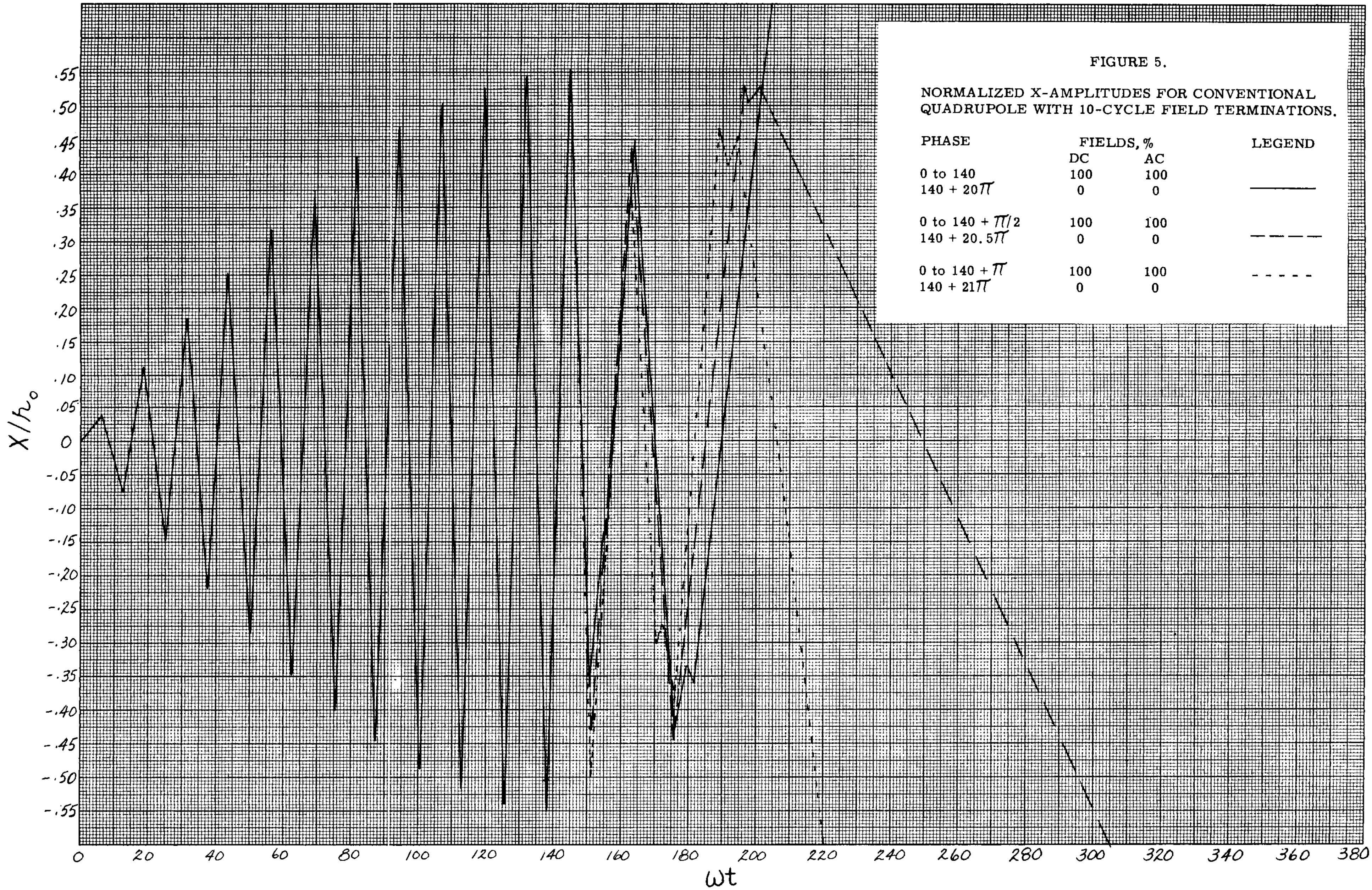

FIGURE 5.
NORMALIZED X-AMPLITUDES FOR CONVENTIONAL QUADRUPOLE WITH 10-CYCLE FIELD TERMINATIONS.
PHASE
FIELDS, %
DC
AC
LEGEND
0 to 140
140 + 20π
100 100
0 0
0 to 140 + π/2
140 + 20.5π
100 100
0 0
0 to 140 + π
140 + 21π
100 100
0 0
X/h₀
.55
.50
.45
.40
.35
.30
.25
.20
.15
.10
.05
0
-.05
-.10
-.15
-.20
-.25
-.30
-.35
-.40
-.45
-.50
-.55
0 20 40 60 80 100 120 140 160 180 200 220 240 260 280 300 320 340 360 380
ωt

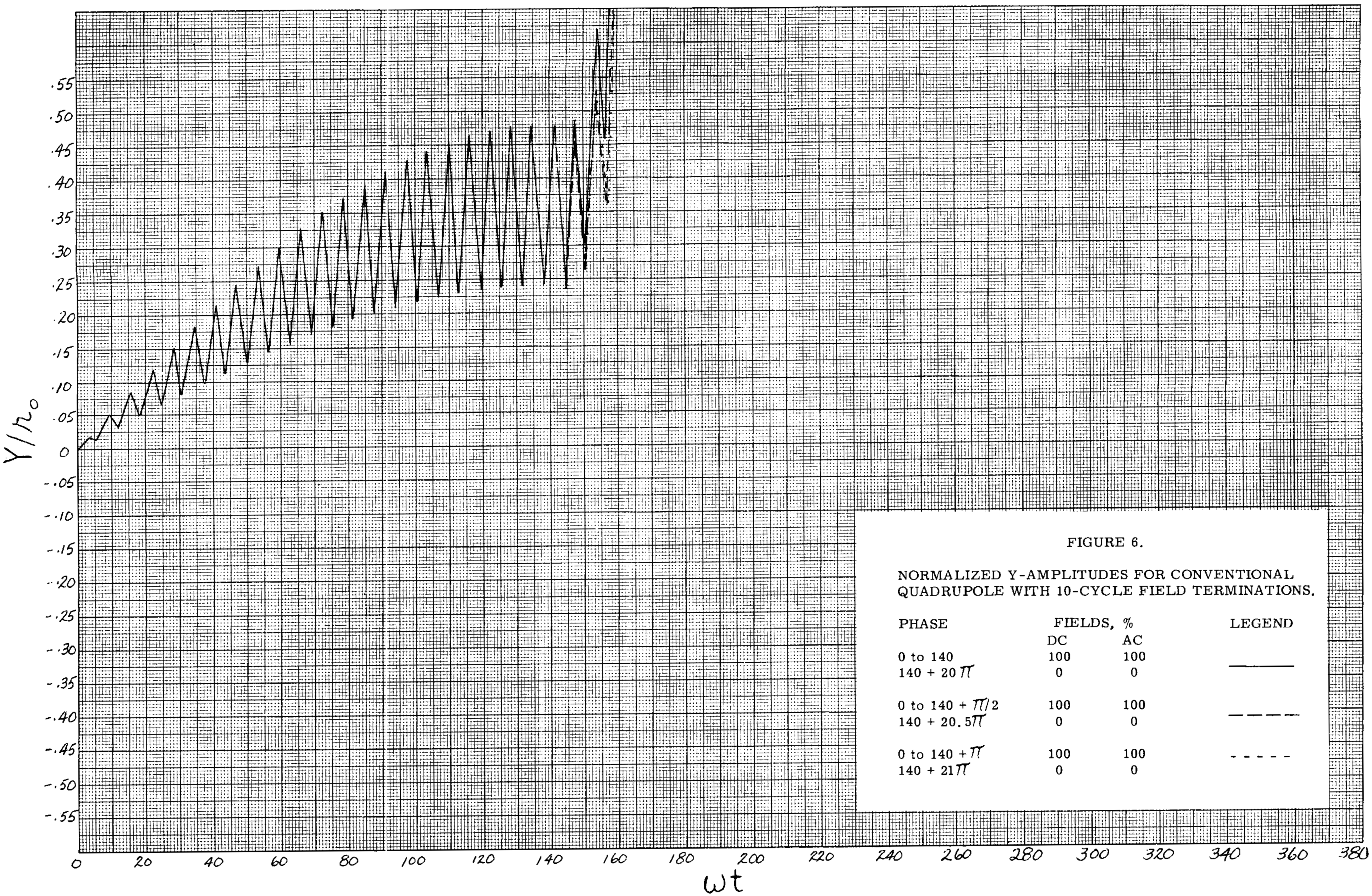

FIGURE 6.

NORMALIZED Y-AMPLITUDES FOR CONVENTIONAL QUADRUPOLE WITH 10-CYCLE FIELD TERMINATIONS.

PHASE	FIELDS, % DC	FIELDS, % AC	LEGEND
0 to 140	100	100	————
$140 + 20\pi$	0	0	
0 to $140 + \pi/2$	100	100	— — — —
$140 + 20.5\pi$	0	0	
0 to $140 + \pi$	100	100	- - - - -
$140 + 21\pi$	0	0	

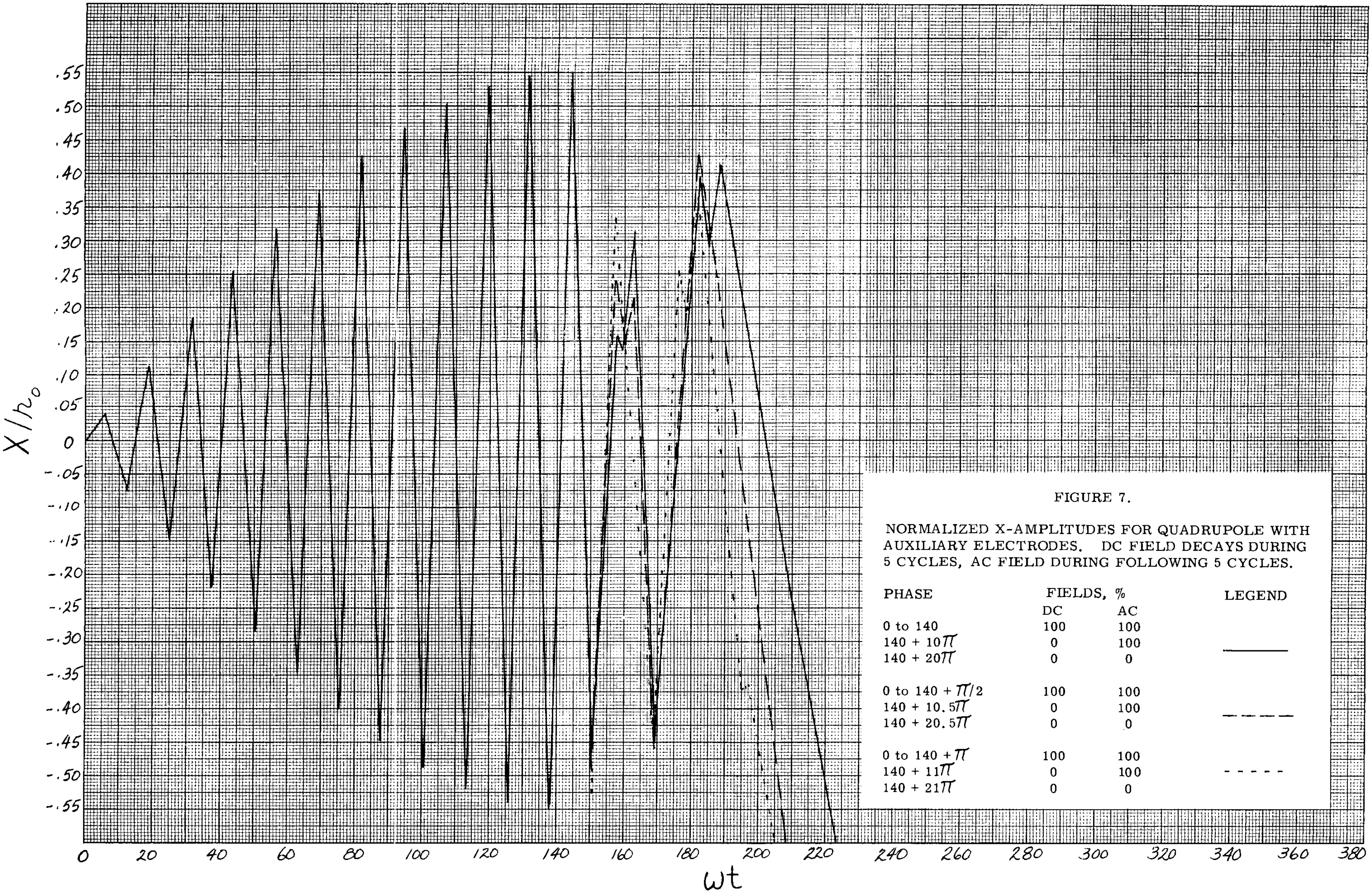
X/r₀
.55
.50
.45
.40
.35
.30
.25
.20
.15
.10
.05
0
-.05
-.10
-.15
-.20
-.25
-.30
-.35
-.40
-.45
-.50
-.55
0 20 40 60 80 100 120 140 160 180 200 220 240 260 280 300 320 340 360 380
ωt
FIGURE 7.
NORMALIZED X-AMPLITUDES FOR QUADRUPOLE WITH AUXILIARY ELECTRODES. DC FIELD DECAYS DURING 5 CYCLES, AC FIELD DURING FOLLOWING 5 CYCLES.
PHASE | FIELDS, % DC | AC | LEGEND
0 to 140 | 100 | 100
140 + 10π | 0 | 100
140 + 20π | 0 | 0
0 to 140 + π/2 | 100 | 100
140 + 10.5π | 0 | 100
140 + 20.5π | 0 | 0
0 to 140 + π | 100 | 100
140 + 11π | 0 | 100
140 + 21π | 0 | 0

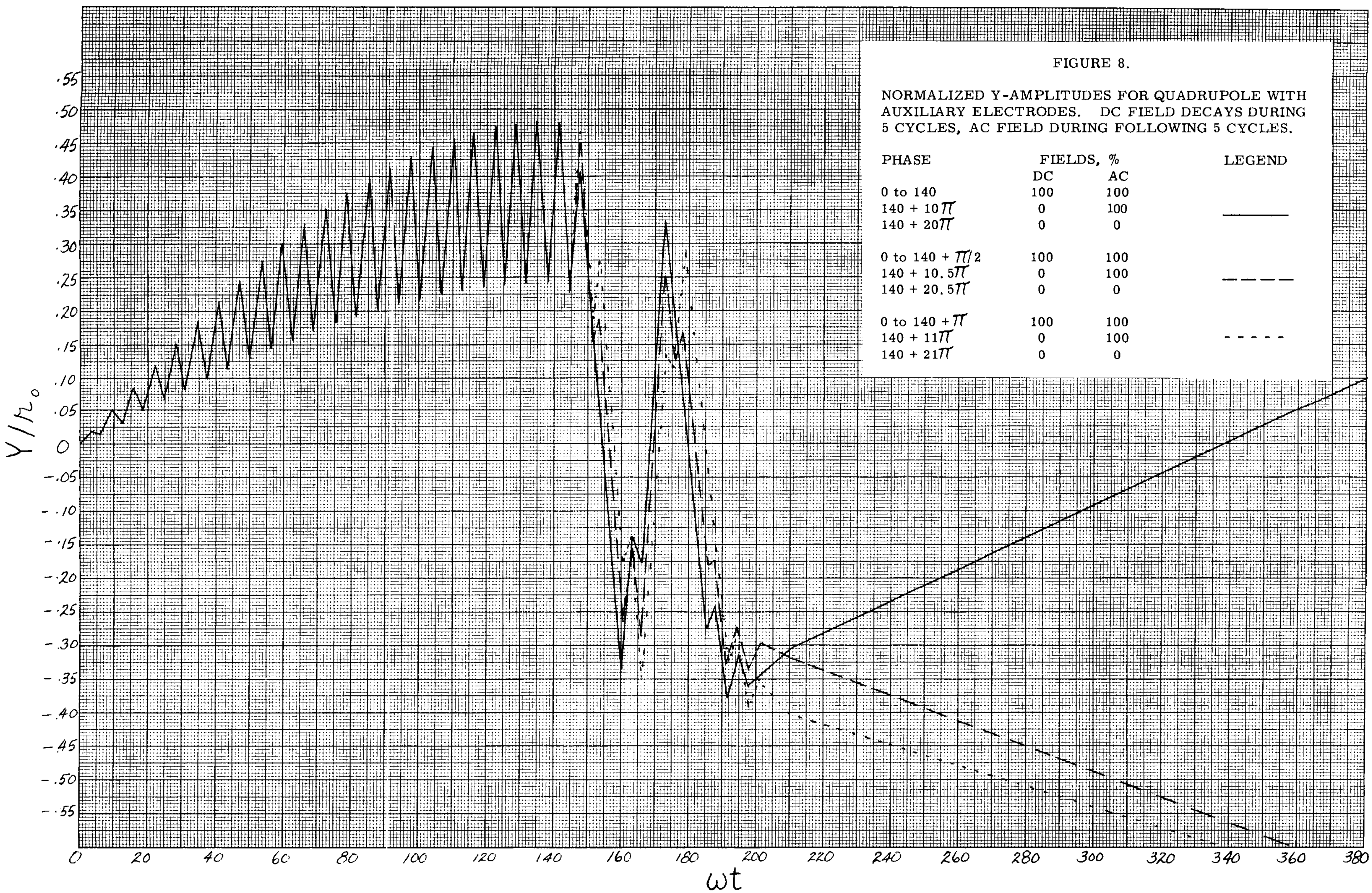

FIGURE 8.

NORMALIZED Y-AMPLITUDES FOR QUADRUPOLE WITH AUXILIARY ELECTRODES. DC FIELD DECAYS DURING 5 CYCLES, AC FIELD DURING FOLLOWING 5 CYCLES.

PHASE	FIELDS, % DC	AC	LEGEND
0 to 140	100	100	
140 + 10π	0	100	———
140 + 20π	0	0	
0 to 140 + π/2	100	100	
140 + 10.5π	0	100	— — —
140 + 20.5π	0	0	
0 to 140 + π	100	100	
140 + 11π	0	100	- - - - -
140 + 21π	0	0	

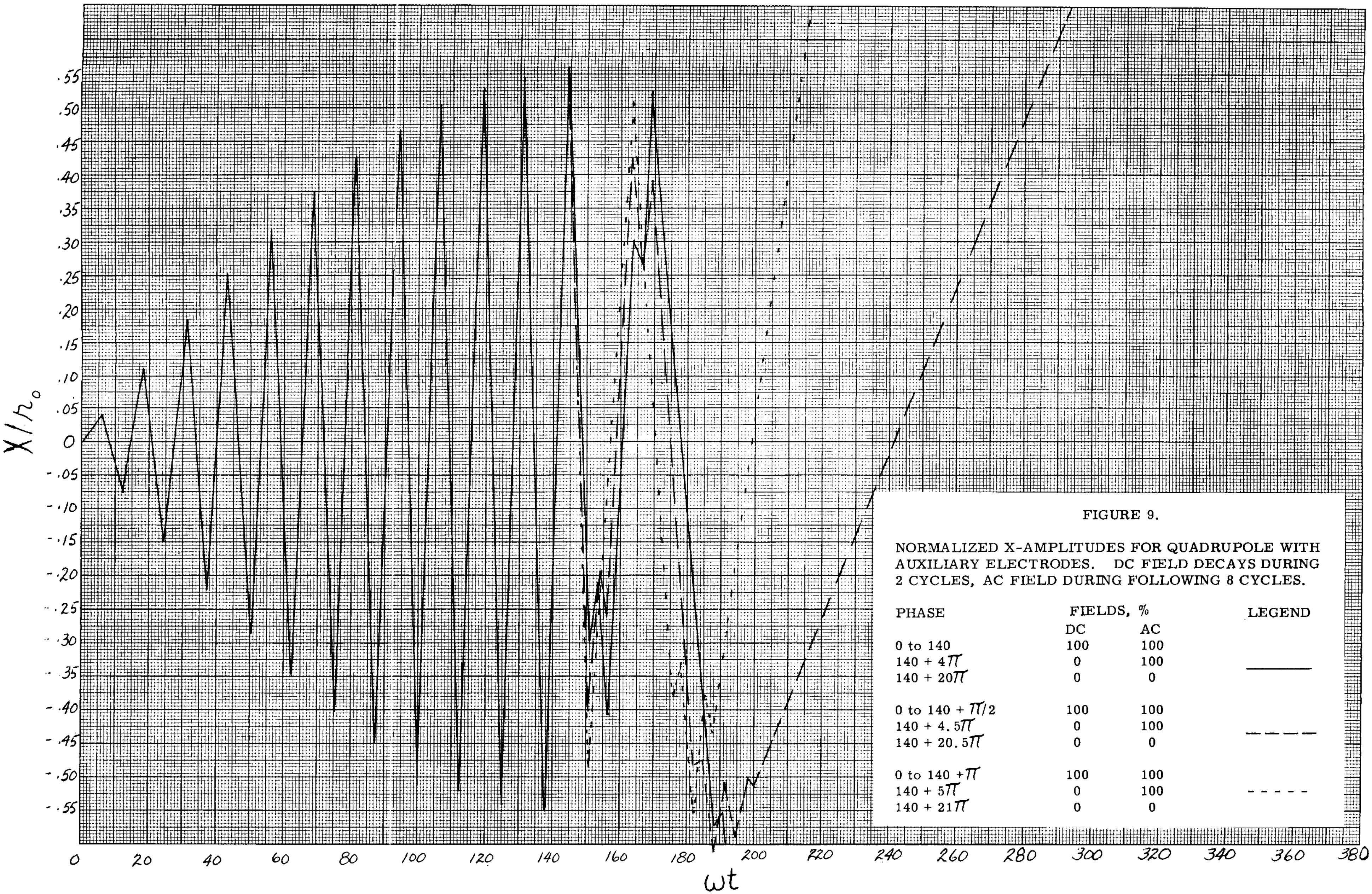

FIGURE 9.

NORMALIZED X-AMPLITUDES FOR QUADRUPOLE WITH AUXILIARY ELECTRODES. DC FIELD DECAYS DURING 2 CYCLES, AC FIELD DURING FOLLOWING 8 CYCLES.

PHASE	FIELDS, % DC	AC	LEGEND
0 to 140	100	100	
140 + 4π	0	100	———
140 + 20π	0	0	
0 to 140 + π/2	100	100	
140 + 4.5π	0	100	— — —
140 + 20.5π	0	0	
0 to 140 + π	100	100	
140 + 5π	0	100	- - - - -
140 + 21π	0	0	

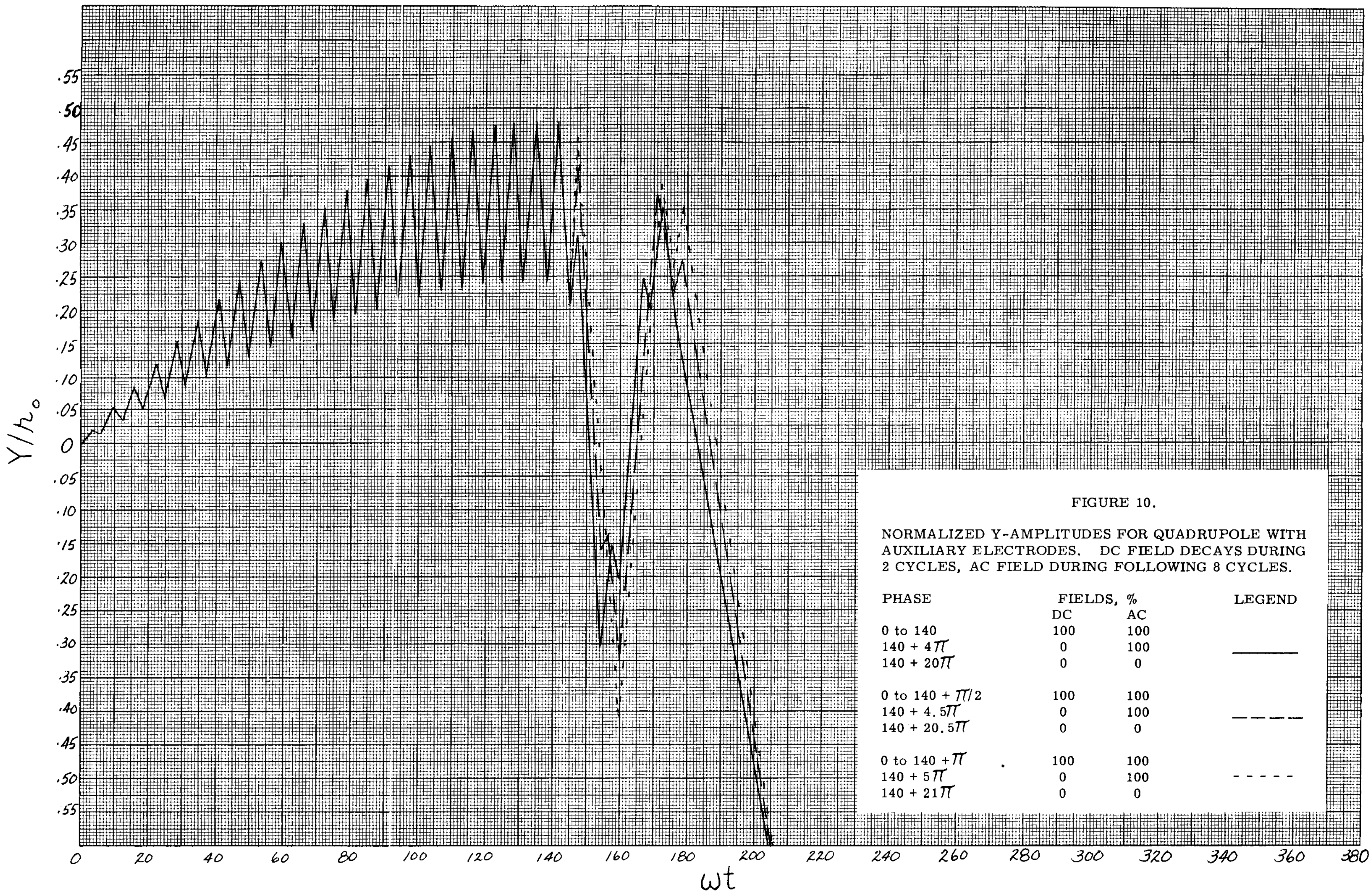

FIGURE 10.

NORMALIZED Y-AMPLITUDES FOR QUADRUPOLE WITH AUXILIARY ELECTRODES. DC FIELD DECAYS DURING 2 CYCLES, AC FIELD DURING FOLLOWING 8 CYCLES.

PHASE	FIELDS, % DC	AC	LEGEND
0 to 140	100	100	
140 + 4π	0	100	———
140 + 20π	0	0	
0 to 140 + $\pi/2$	100	100	
140 + 4.5π	0	100	— — —
140 + 20.5π	0	0	
0 to 140 + π	100	100	
140 + 5π	0	100	- - - - -
140 + 21π	0	0	

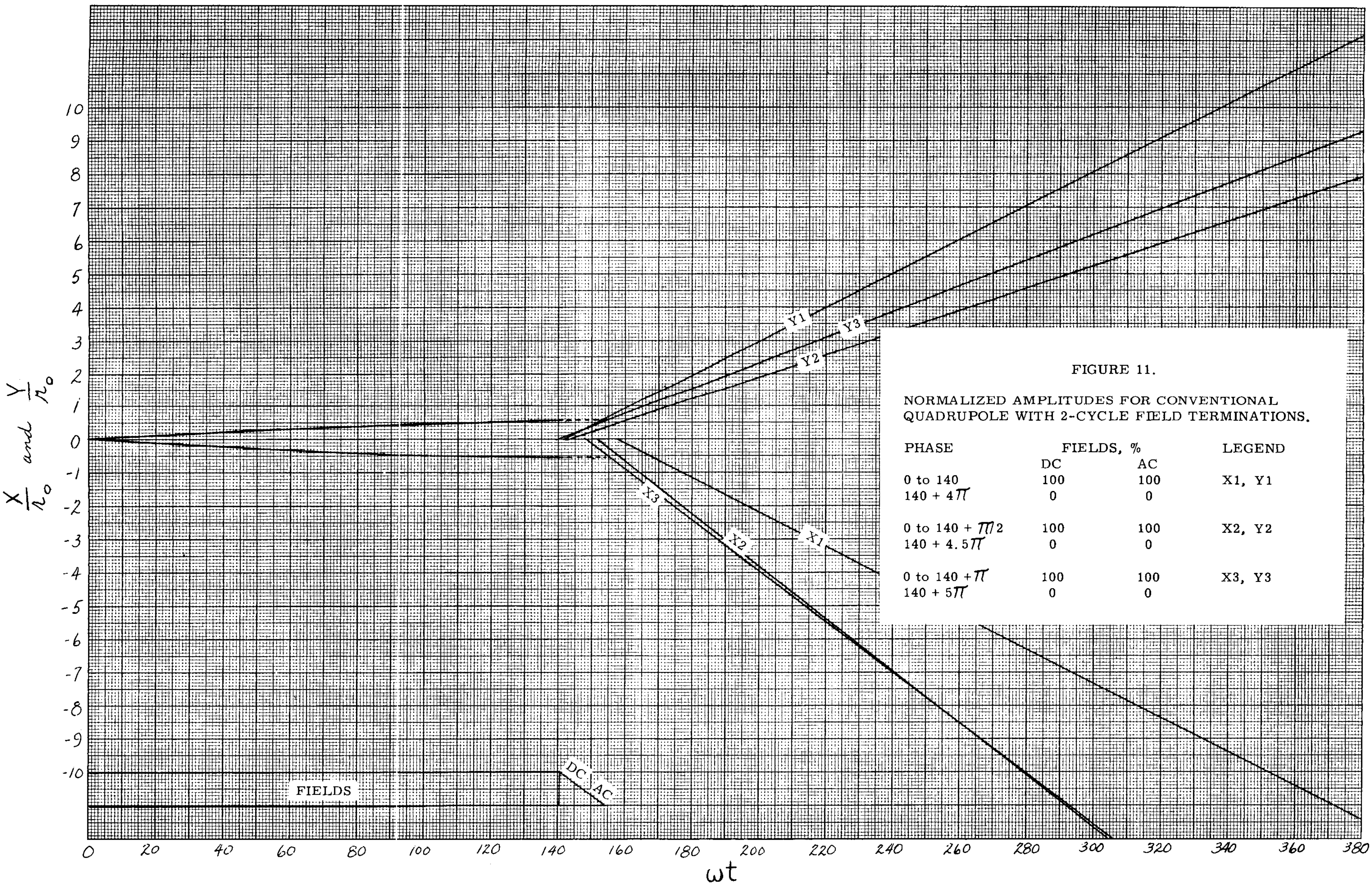

FIGURE 11.

NORMALIZED AMPLITUDES FOR CONVENTIONAL QUADRUPOLE WITH 2-CYCLE FIELD TERMINATIONS.

PHASE	FIELDS, % DC	FIELDS, % AC	LEGEND
0 to 140	100	100	X1, Y1
140 + 4π	0	0	
0 to 140 + $\pi/2$	100	100	X2, Y2
140 + 4.5π	0	0	
0 to 140 + π	100	100	X3, Y3
140 + 5π	0	0	

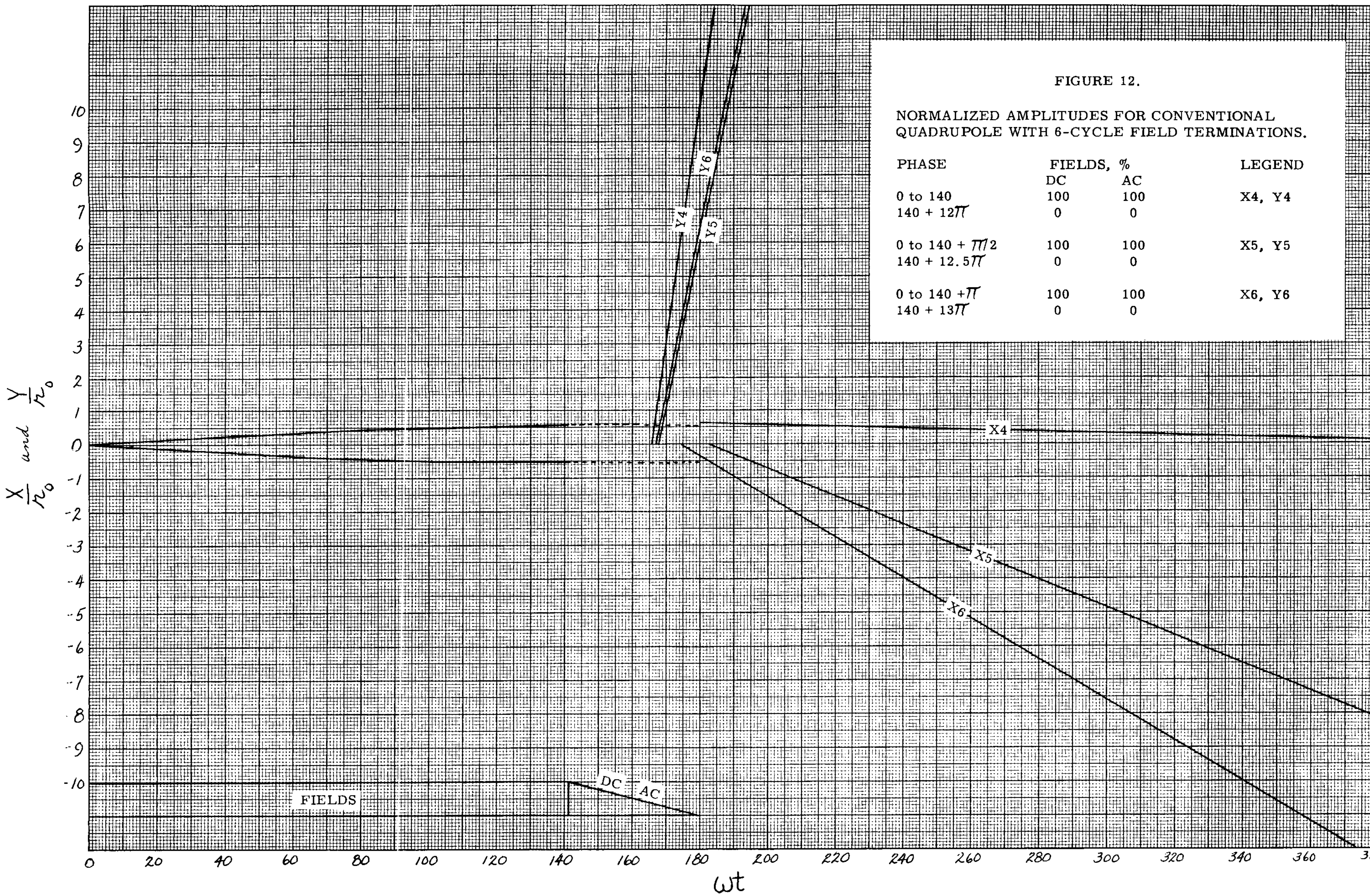

FIGURE 12.

NORMALIZED AMPLITUDES FOR CONVENTIONAL QUADRUPOLE WITH 6-CYCLE FIELD TERMINATIONS.

PHASE	FIELDS, % DC	AC	LEGEND
0 to 140	100	100	X4, Y4
140 + 12π	0	0	
0 to 140 + π/2	100	100	X5, Y5
140 + 12.5π	0	0	
0 to 140 +π	100	100	X6, Y6
140 + 13π	0	0	

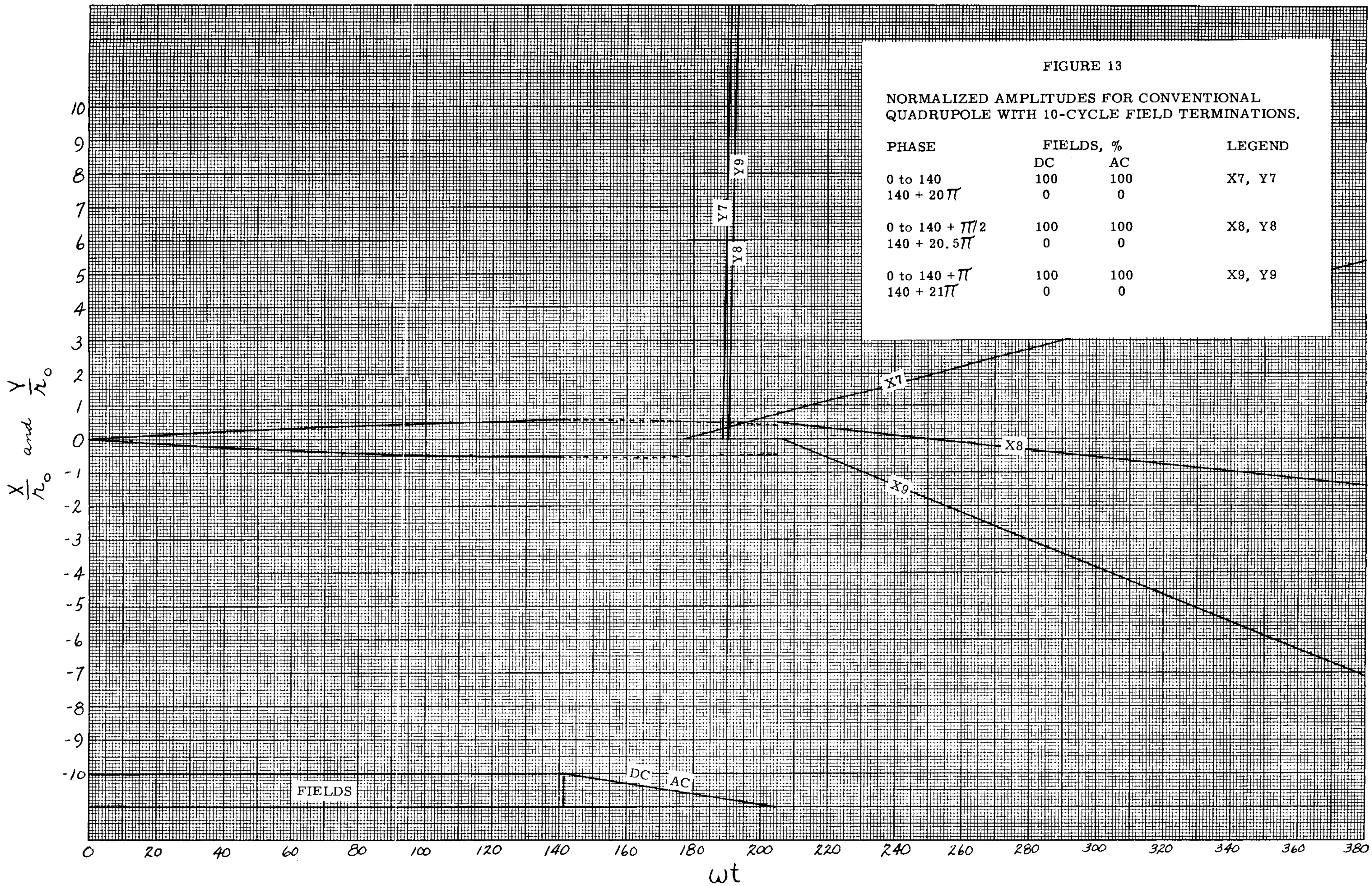
FIGURE 13
NORMALIZED AMPLITUDES FOR CONVENTIONAL QUADRUPOLE WITH 10-CYCLE FIELD TERMINATIONS.
PHASE
FIELDS, %
DC
AC
LEGEND
0 to 140
100
100
X7, Y7
140 + 20π
0
0
0 to 140 + π/2
100
100
X8, Y8
140 + 20.5π
0
0
0 to 140 + π
100
100
X9, Y9
140 + 21π
0
0
Y9
Y7
Y8
X7
X8
X9
DC
AC
FIELDS
X/r₀ and Y/r₀
ωt

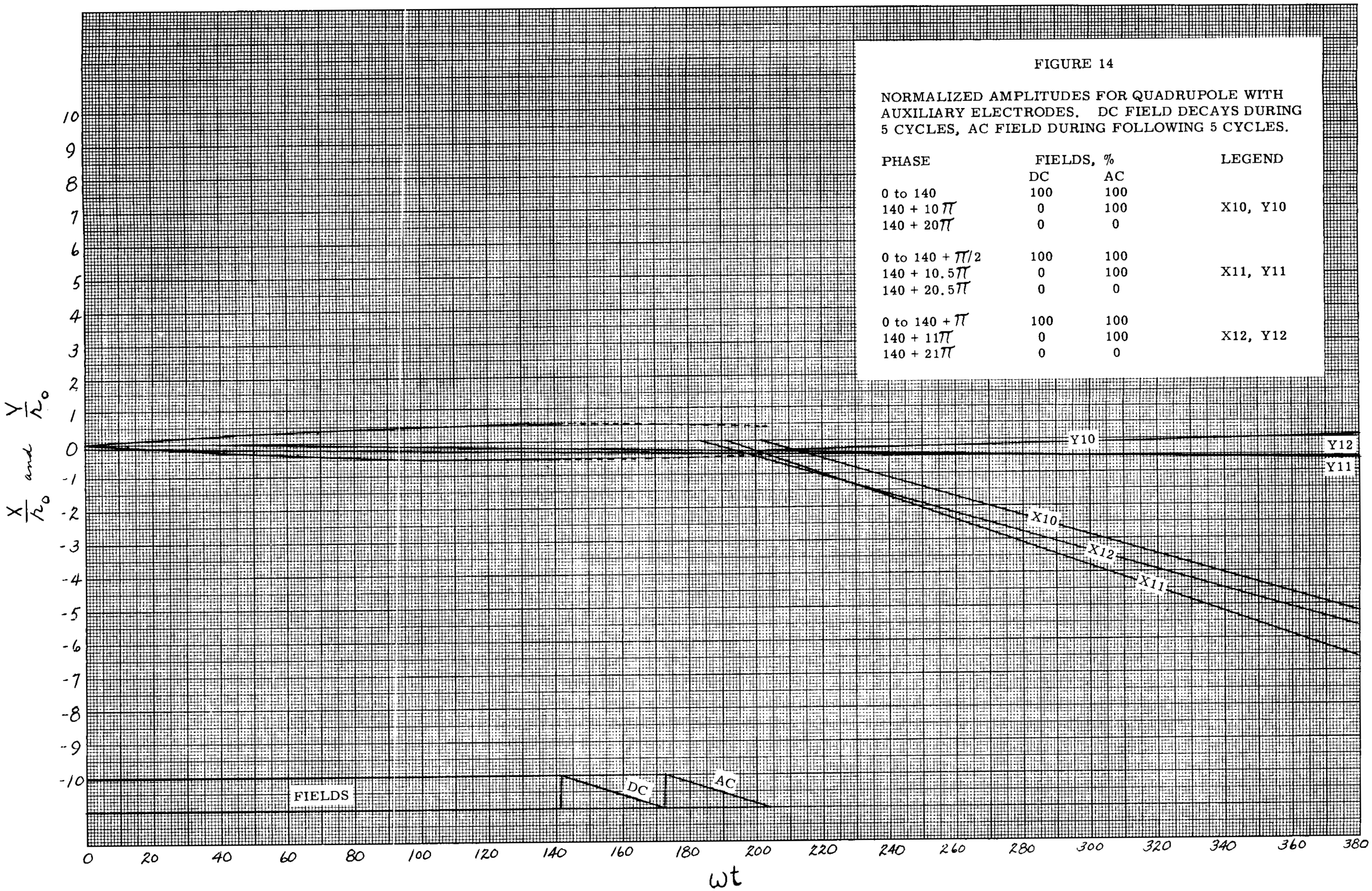

FIGURE 14

NORMALIZED AMPLITUDES FOR QUADRUPOLE WITH AUXILIARY ELECTRODES. DC FIELD DECAYS DURING 5 CYCLES, AC FIELD DURING FOLLOWING 5 CYCLES.

PHASE	FIELDS, % DC	AC	LEGEND
0 to 140	100	100	
140 + 10π	0	100	X10, Y10
140 + 20π	0	0	
0 to 140 + π/2	100	100	
140 + 10.5π	0	100	X11, Y11
140 + 20.5π	0	0	
0 to 140 + π	100	100	
140 + 11π	0	100	X12, Y12
140 + 21π	0	0	

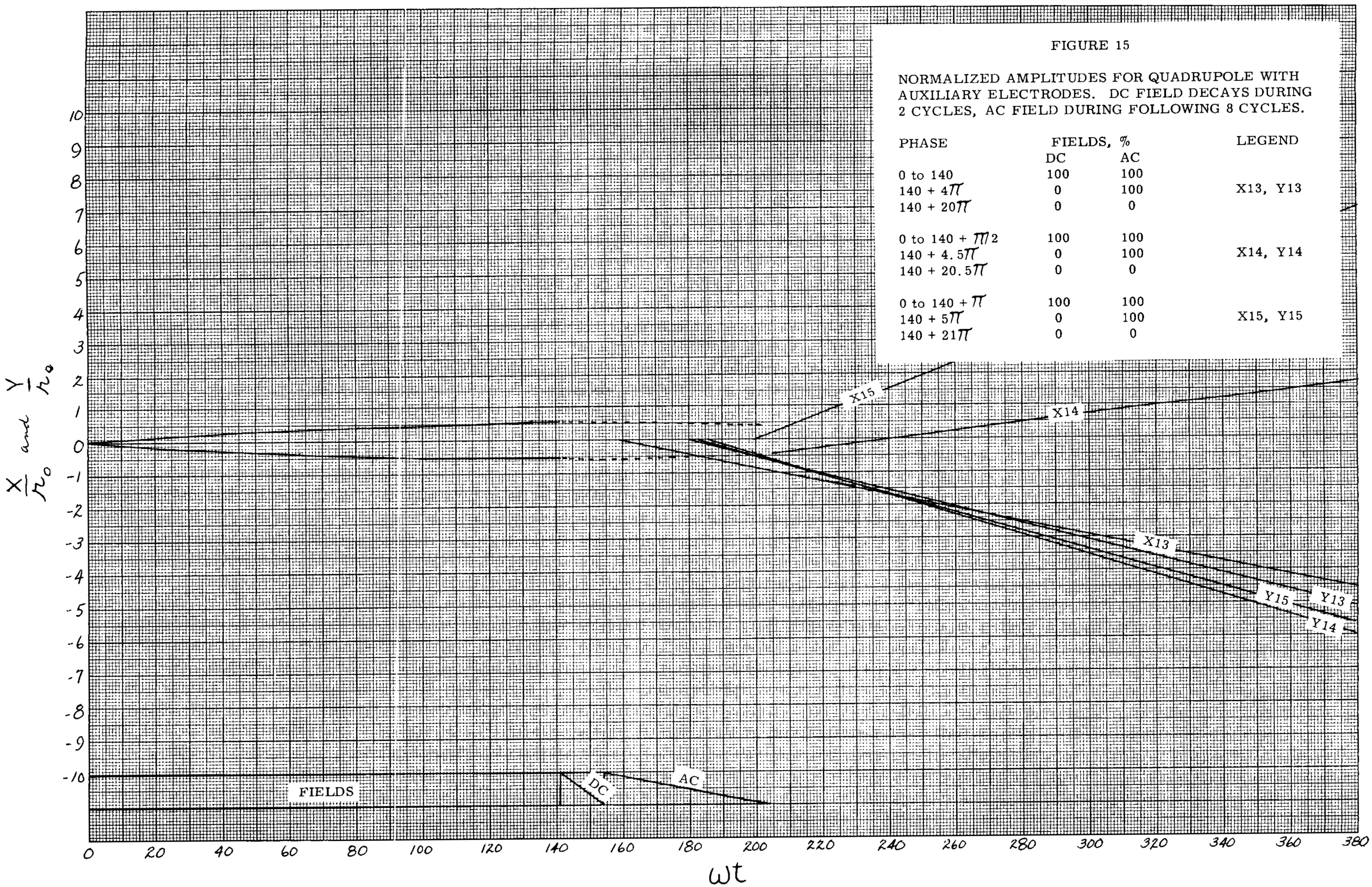

FIGURE 15

NORMALIZED AMPLITUDES FOR QUADRUPOLE WITH AUXILIARY ELECTRODES. DC FIELD DECAYS DURING 2 CYCLES, AC FIELD DURING FOLLOWING 8 CYCLES.

PHASE	FIELDS, % DC	AC	LEGEND
0 to 140	100	100	
$140 + 4\pi$	0	100	X13, Y13
$140 + 20\pi$	0	0	
0 to $140 + \pi/2$	100	100	
$140 + 4.5\pi$	0	100	X14, Y14
$140 + 20.5\pi$	0	0	
0 to $140 + \pi$	100	100	
$140 + 5\pi$	0	100	X15, Y15
$140 + 21\pi$	0	0	

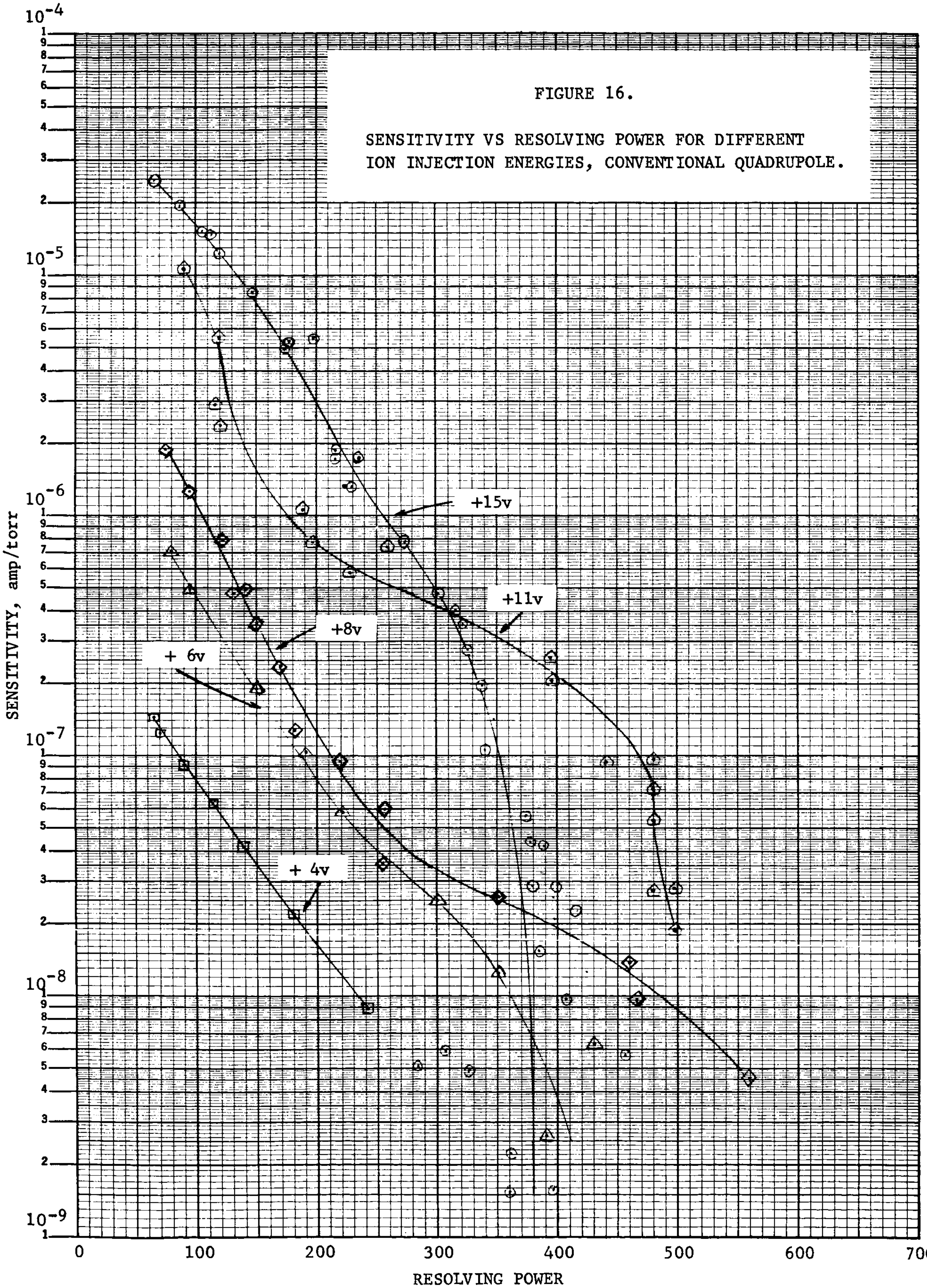
FIGURE 16.
SENSITIVITY VS RESOLVING POWER FOR DIFFERENT ION INJECTION ENERGIES, CONVENTIONAL QUADRUPOLE.
+15v
+11v
+8v
+ 6v
+ 4v
SENSITIVITY, amp/torr
10^{-4}
10^{-5}
10^{-6}
10^{-7}
10^{-8}
10^{-9}
0
100
200
300
400
500
600
700
RESOLVING POWER

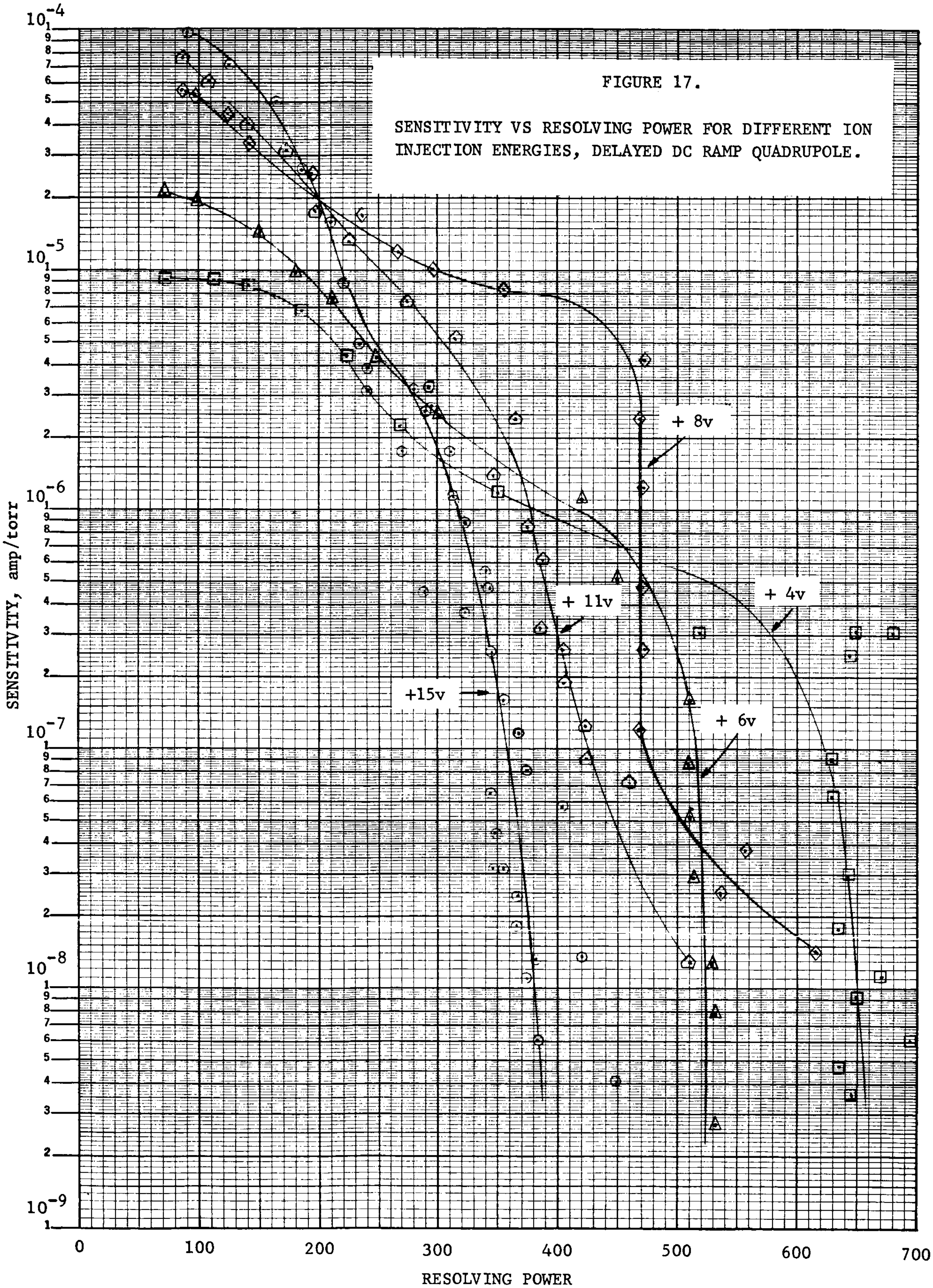

FIGURE 17.
SENSITIVITY VS RESOLVING POWER FOR DIFFERENT ION INJECTION ENERGIES, DELAYED DC RAMP QUADRUPOLE.
+ 8v
+ 11v
+ 4v
+15v
+ 6v
SENSITIVITY, amp/torr
RESOLVING POWER
0
100
200
300
400
500
600
700

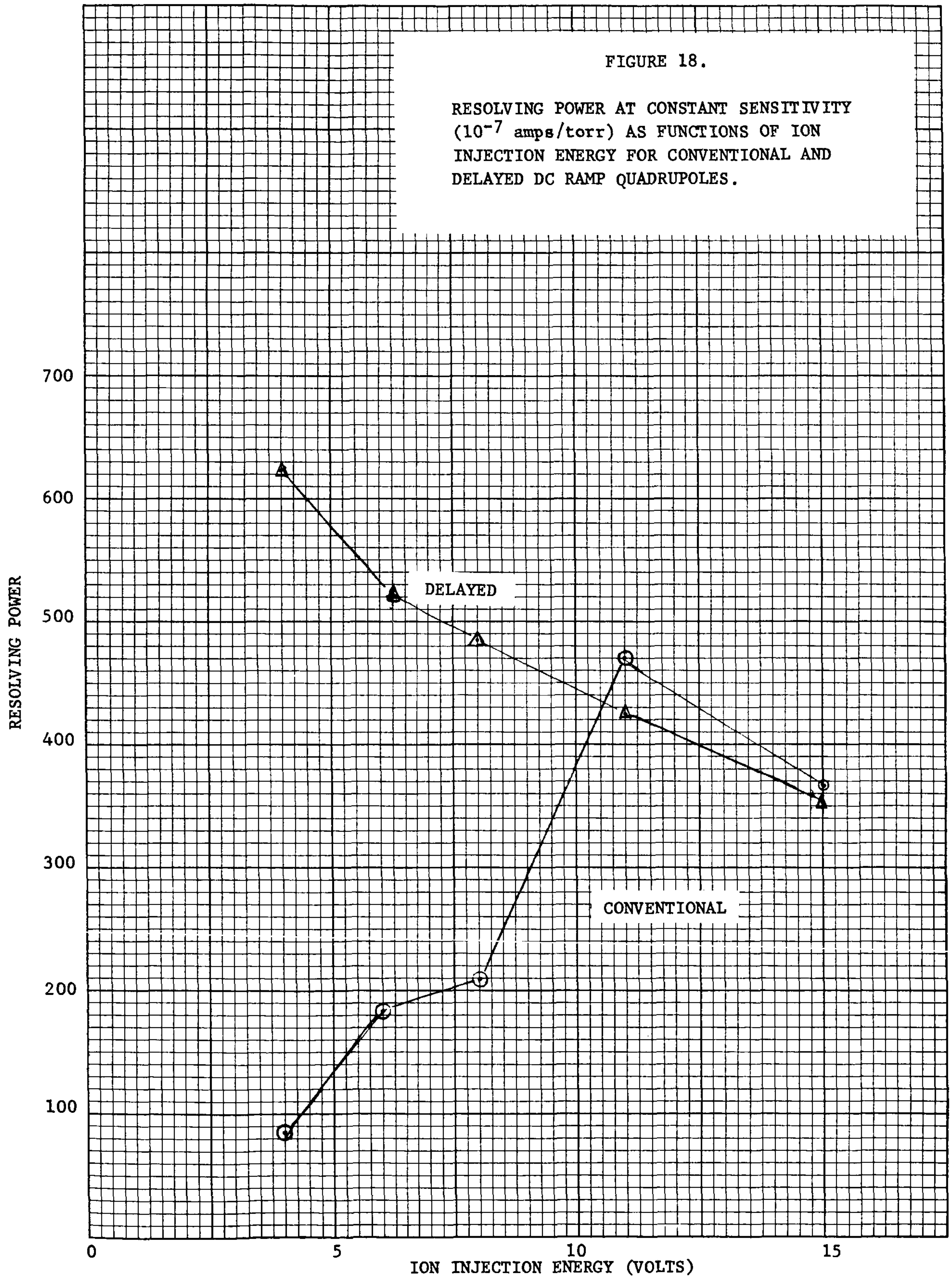

FIGURE 18.
RESOLVING POWER AT CONSTANT SENSITIVITY
(10^{-7} amps/torr) AS FUNCTIONS OF ION
INJECTION ENERGY FOR CONVENTIONAL AND
DELAYED DC RAMP QUADRUPOLES.
DELAYED
CONVENTIONAL
RESOLVING POWER
700
600
500
400
300
200
100
0
5
10
15
ION INJECTION ENERGY (VOLTS)

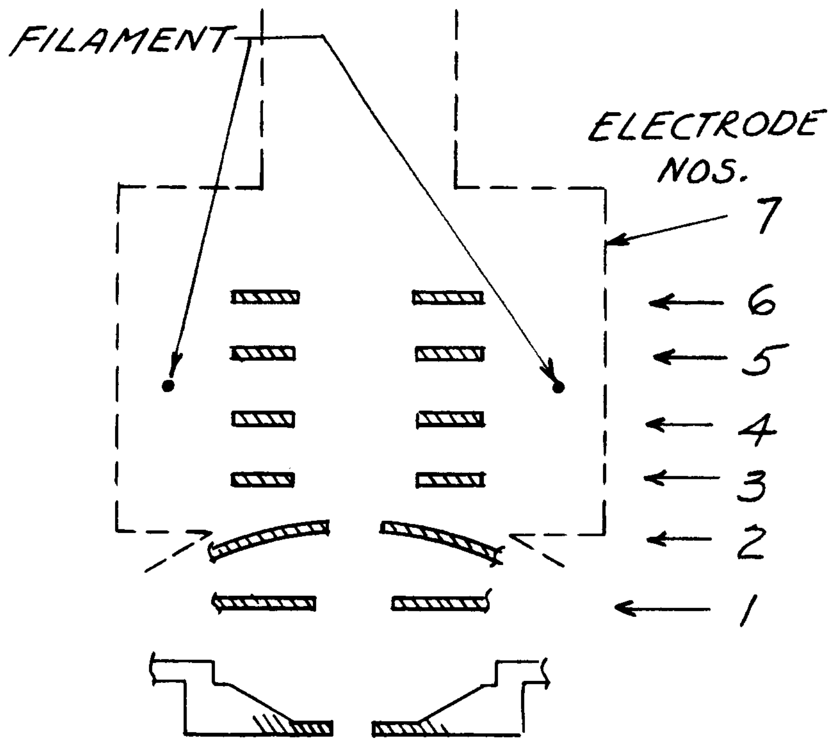

ION SOURCE

FIGURE 19

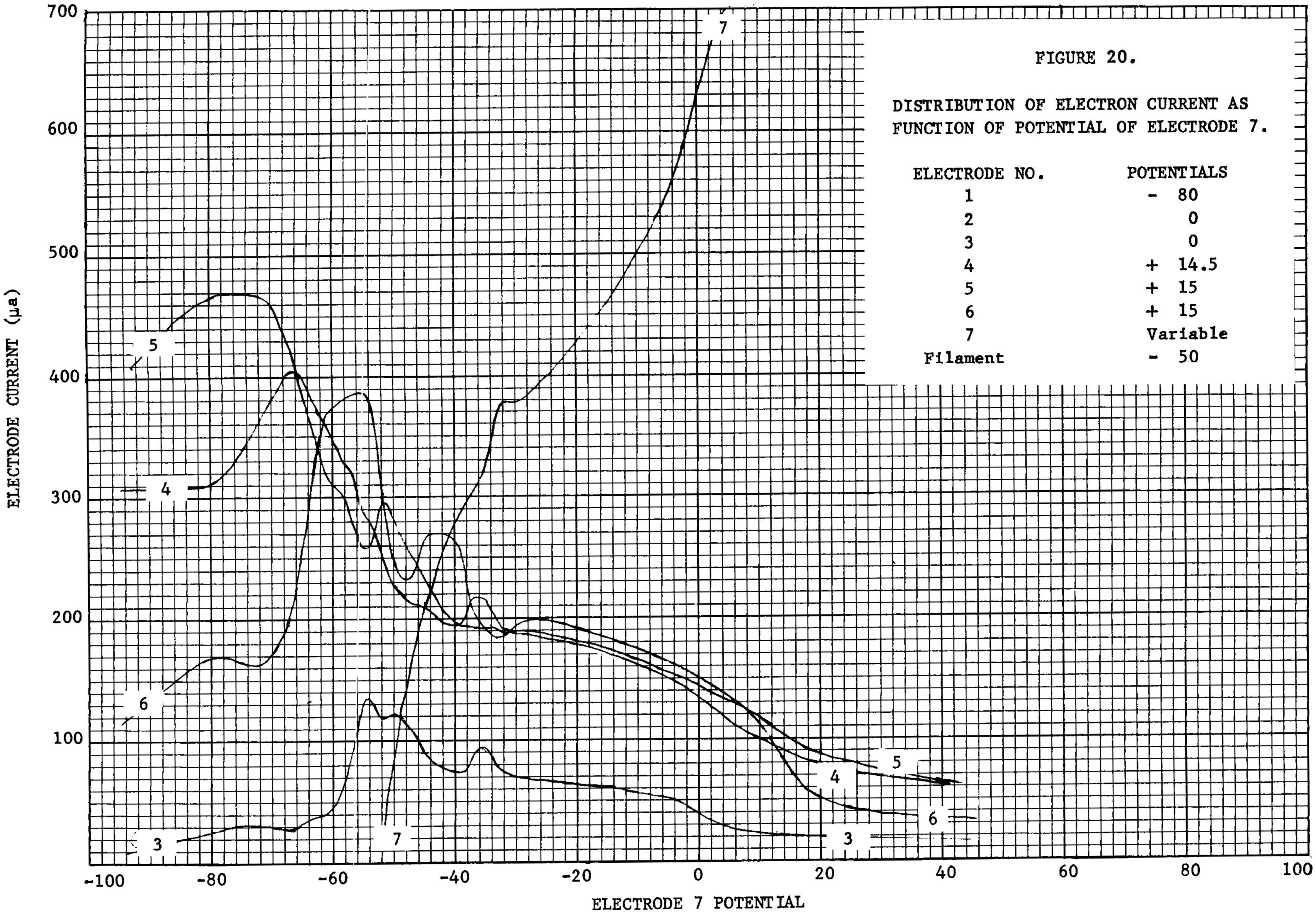

FIGURE 20.

DISTRIBUTION OF ELECTRON CURRENT AS FUNCTION OF POTENTIAL OF ELECTRODE 7.

ELECTRODE NO.	POTENTIALS
1	- 80
2	0
3	0
4	+ 14.5
5	+ 15
6	+ 15
7	Variable
Filament	- 50

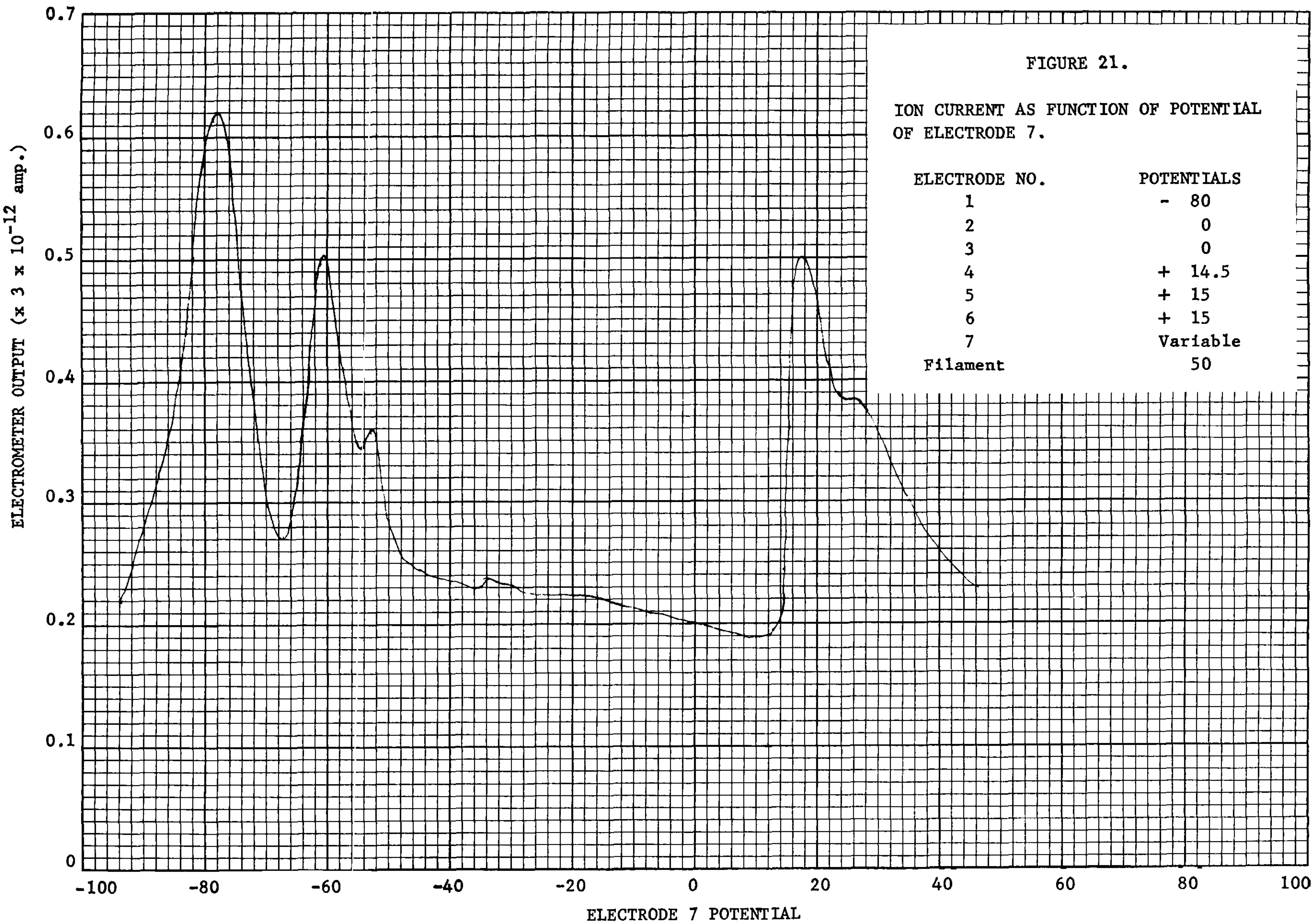

FIGURE 21.

ION CURRENT AS FUNCTION OF POTENTIAL OF ELECTRODE 7.

ELECTRODE NO.	POTENTIALS
1	- 80
2	0
3	0
4	+ 14.5
5	+ 15
6	+ 15
7	Variable
Filament	50

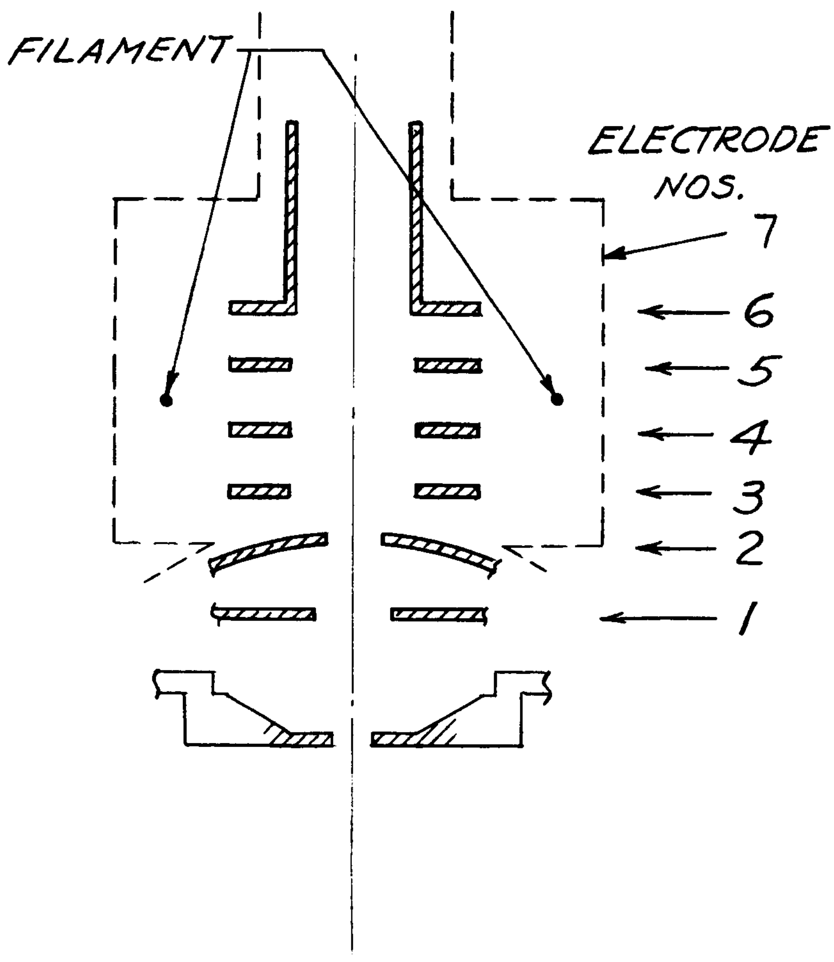

IMPROVED ION SOURCE

FIGURE 22

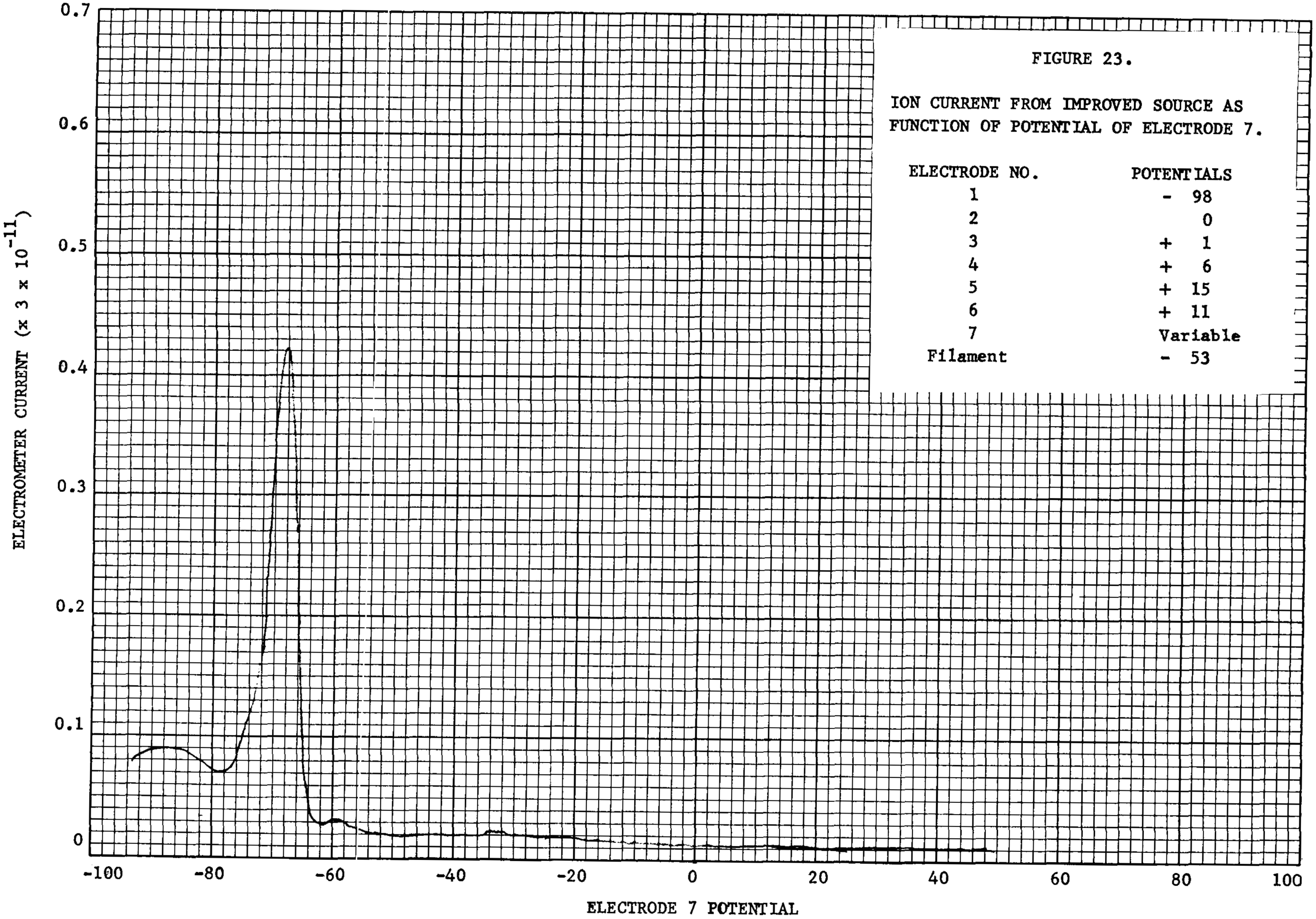

FIGURE 23.

ION CURRENT FROM IMPROVED SOURCE AS FUNCTION OF POTENTIAL OF ELECTRODE 7.

ELECTRODE NO.	POTENTIALS
1	- 98
2	0
3	+ 1
4	+ 6
5	+ 15
6	+ 11
7	Variable
Filament	- 53

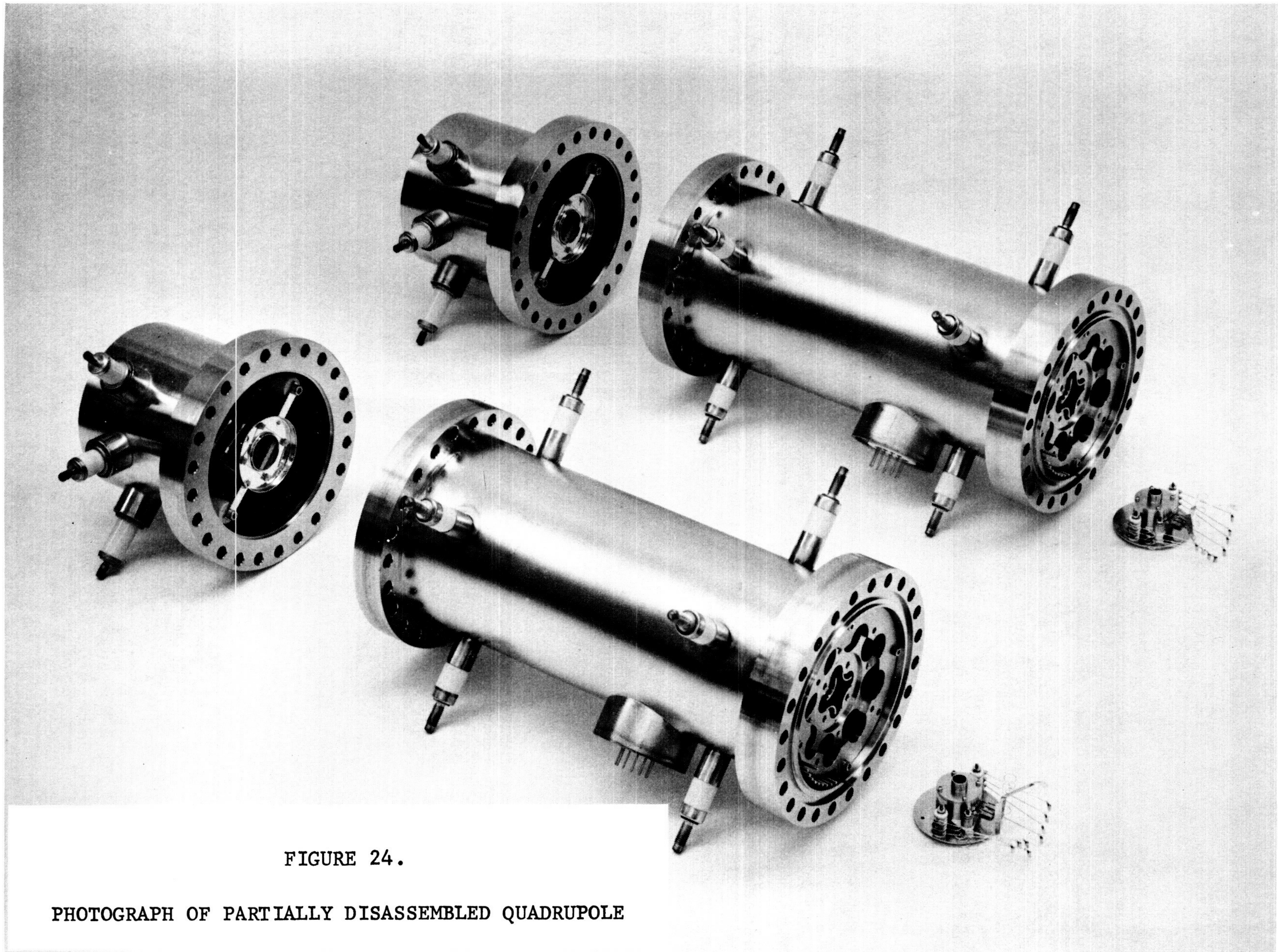

FIGURE 24.

PHOTOGRAPH OF PARTIALLY DISASSEMBLED QUADRUPOLE

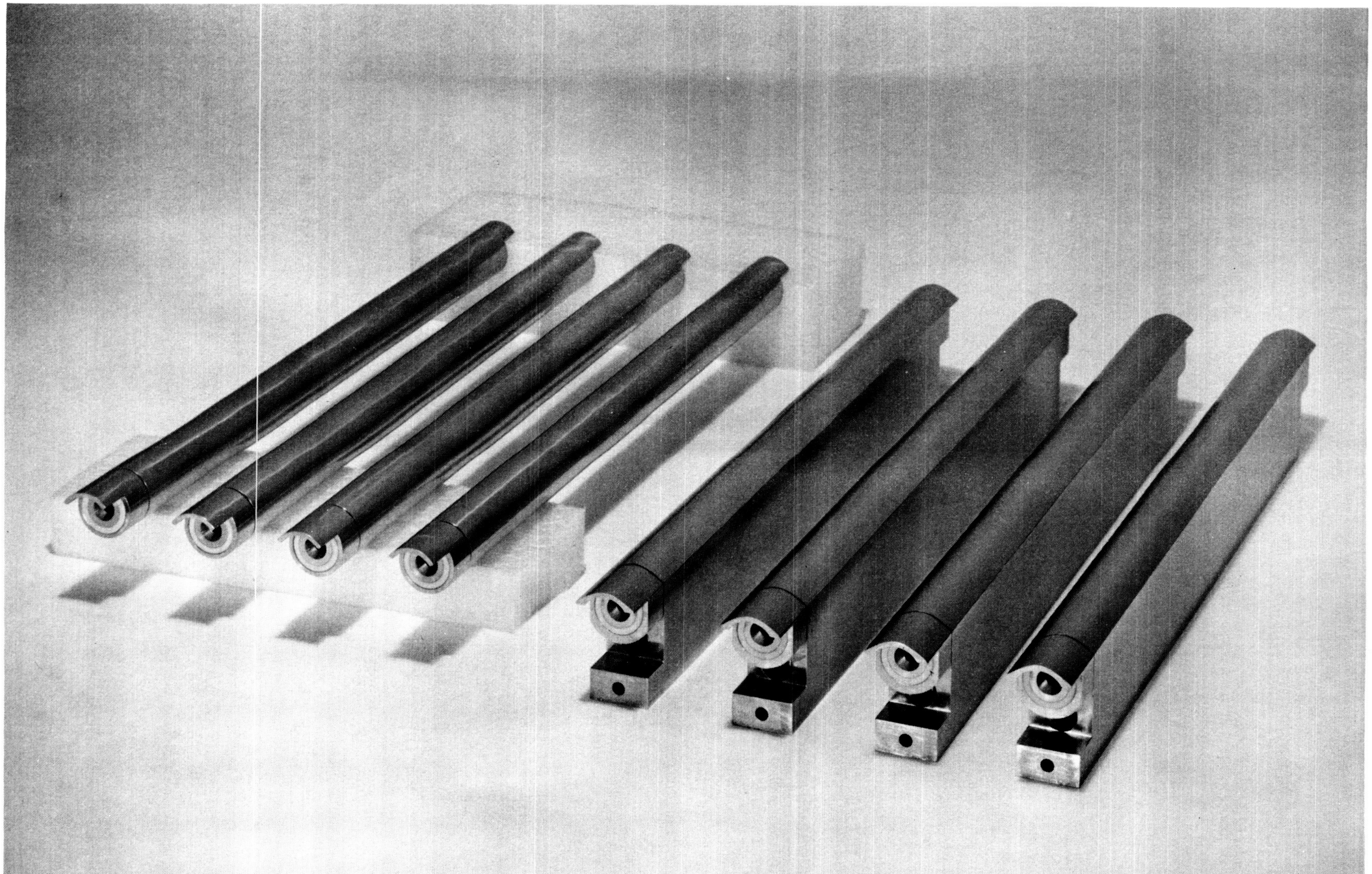

FIGURE 25.

PHOTOGRAPH OF ROUND AND HYPERBOLIC ROD SETS.

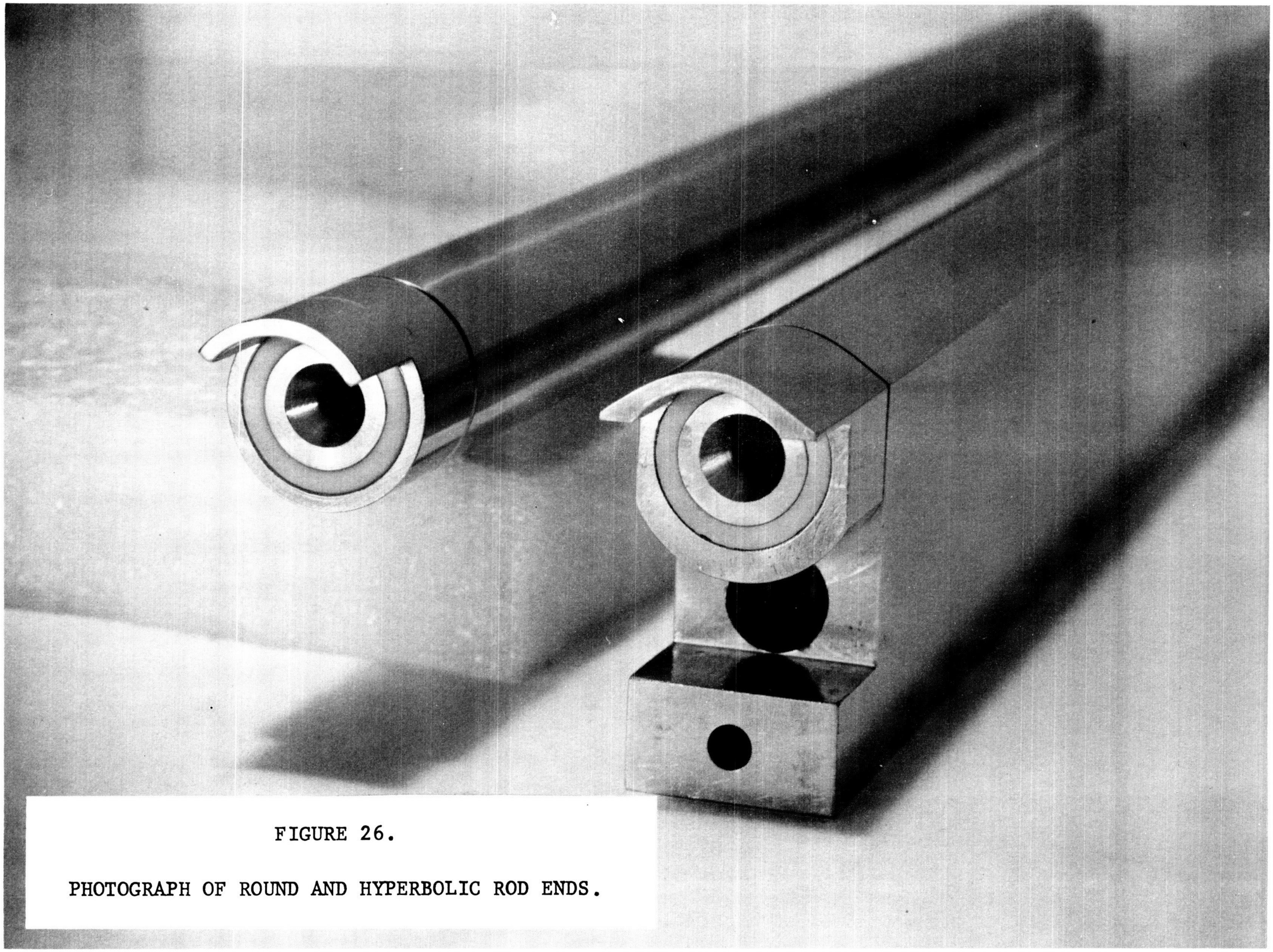

FIGURE 26.

PHOTOGRAPH OF ROUND AND HYPERBOLIC ROD ENDS.

APPENDIX

Abstract of paper presented at the meeting of
the American Vacuum Society in San Francisco,
October, 1966

IMPROVED QUADRUPOLE MASS FILTER

Wilson M. Brubaker

Bell & Howell Research Center
Pasadena, California

The transmission of ions through a conventional quadrupole mass filter is severely attenuated by the impulses which the ions receive as they traverse the fringing field. A computer study has been made to evaluate this phenomenon. Serious losses are indicated. The computer was also used to explore the effectiveness of a proposed scheme for eliminating these undesired radially directed impulses. The results of the computer study were encouraging, and an experimental apparatus was built to evaluate the scheme in the laboratory. Preliminary results indicate that, at the higher resolving powers, the transmission of ions through the quadrupole is increased by factors of ten to one hundred by the use of this refinement. This increased transmission is obtained without loss of resolving power.

This work was supported in part by NASA under Contract No. NASW-1298